Report on model parameterization
-
Normal evolution scenario

OPERA-PU-NRG7251-NES

Radioactive substances and ionizing radiation are used in medicine, industry, agriculture, research, education and electricity production. This generates radioactive waste. In the Netherlands, this waste is collected, treated and stored by COVRA (Centrale Organisatie Voor Radioactief Afval). After interim storage for a period of at least 100 years radioactive waste is intended for disposal. There is a worldwide scientific and technical consensus that geological disposal represents the safest long-term option for radioactive waste.

Geological disposal is emplacement of radioactive waste in deep underground formations. The goal of geological disposal is long-term isolation of radioactive waste from our living environment in order to avoid exposure of future generations to ionising radiation from the waste. OPERA (OnderzoeksProgramma Eindberging Radioactief Afval) is the Dutch research programme on geological disposal of radioactive waste.

Within OPERA, researchers of different organisations in different areas of expertise will cooperate on the initial, conditional Safety Cases for the host rocks Boom Clay and Zechstein rock salt. As the radioactive waste disposal process in the Netherlands is at an early, conceptual phase and the previous research programme has ended more than a decade ago, in OPERA a first preliminary or initial safety case will be developed to structure the research necessary for the eventual development of a repository in the Netherlands. The safety case is conditional since only the long-term safety of a generic repository will be assessed. OPERA is financed by the Dutch Ministry of Economic Affairs and the public limited liability company Electriciteits-Produktiemaatschappij Zuid-Nederland (EPZ) and coordinated by COVRA. Further details on OPERA and its outcomes can be accessed at www.covra.nl.

This report concerns a study conducted in the framework of OPERA. The conclusions and viewpoints presented in the report are those of the author(s). COVRA may draw modified conclusions, based on additional literature sources and expert opinions. A .pdf version of this document can be downloaded from www.covra.nl.

OPERA-PU-NRG7251-NES
Title: Report on model parameterization - Normal evolution scenario
Authors: T.J. Schröder, J. Hart, J.C.L. Meeussen
Date of publication: 12 September 2017 (Revision 1)
Keywords: Safety Case, safety assessment, model parameters

Contents

List of figures

List of tables

Summary

The main objective of the OPERA research programme is to provide tools and data for the development of Safety Cases for national repository concepts for radioactive waste disposals in two host rocks present in the Netherlands, rock salt and Boom Clay.

A central aspect of the Safety Case is the execution of a safety assessment. Within the OPERA research programme, a generic safety assessment is being performed that evaluates all safety relevant aspects of the OPERA disposal concept in Boom Clay and will assess the long-term safety of such a facility. The safety assessment will be carried out for scenarios relevant for the assessment of the long-term safety of a repository in Boom Clay.

The scenarios defined in OPERA Task 7.1.1 are translated into physical and geochemical model representations used for the safety assessment, and the relevant processes are defined and parameterization for each scenario on basis of the input of other OPERA WPs.

OPERA Task 7.2.5, *Parameterization of PA models*, is responsible for defining a set of model representations of relevant processes, the accompanying parameter values and their distributions. The models, parameters and their distributions in this report are defined for the *Normal evolution scenario*.

The objective of the present report is to define a list of input parameters for the *Normal evolution scenario* as well as their values that are required for the ORCHESTRA computer code to perform the OPERA safety assessment, both for the reference scenario and the alternative scenarios. The lists of input parameters are based on guidelines from the experts in Work Packages 3 to 6 to provide numerical values and/or model descriptions for the required data.

Samenvatting

De belangrijkste doelstelling van het OPERA programma is de ontwikkeling van Safety Cases voor de Nederlandse eindbergingsconcepten voor radioactief afval in de gastgesteentes steenzout en Boomse Klei.

Een essentieel onderdeel van de Safety Case betreft de veiligheidsstudie, de zogenoemde “Safety Assessment”. Binnen het OPERA programma wordt een generieke veiligheidsstudie gedaan waarbinnen de veiligheids-relevante aspecten van het OPERA eindbergingsconcept in Boomse Klei worden geëvalueerd en de lange-termijn veiligheid wordt beoordeeld. De veiligheidsevaluatie wordt verricht voor alle scenario’s die relevant zijn voor de lange-termijn veiligheid van een eindbergingsfaciliteit in Boomse Klei.

De scenario’s die zijn gedefinieerd in OPERA Taak 7.1.1, zijn vertaald in fysische en chemische modelrepresentaties voor de veiligheidsevaluatie, en voor elk scenario de relevante processen zijn geparametriseerd op basis van de input van andere OPERA werkpakketten.

OPERA Task 7.2.5, *Parameterization of PA models*, is verantwoordelijk voor het definiëren van modelrepresentaties van de relevante processen, de bijbehorende parameterwaarden en hun kansdichtheidsverdelingen. De modellen, parameters en hun verdelingen zijn voor het *Normale evolutie scenario* gedefinieerd.

Het doel van dit rapport is het definiëren van parameters voor het *Normale evolutie scenario* en hun numerieke waarden die benodigd zijn voor de invoer van het ORCHESTRA rekenprogramma waarmee de OPERA veiligheidsberekeningen zullen worden verricht, voor zowel het referentiescenario als de alternatieve evolutiescenario’s. De waarden van de invoerparameters zijn gebaseerd op richtlijnen van de experts in OPERA Werkpakketten 3

tot 6 ter bepaling van de numerieke waarden en / of modelbeschrijvingen voor de benodigde data.

1. Introduction

1.1. Background

The main objective of the OPERA research programme is to provide tools and data for the development of Safety Cases for national repository concepts for radioactive waste disposals in two host rocks present in the Netherlands, rock salt and Boom Clay [Verhoef, 2011; p.6]. Within the OPERA context, the Safety Case has been explained as a collection of arguments in support of the long-term safety of the repository Clay [Verhoef, 2011; p.5]. A Safety Case comprises the findings (of a safety assessment) and a statement of confidence in these findings.

A central aspect of the Safety Case is the execution of a safety assessment. Within the OPERA research programme, a generic safety assessment is being performed that evaluates all safety relevant aspects of the disposal concept (design of repository) and will assess the long-term safety of such a facility [Verhoef, 2011; p.5].

The execution of a safety assessment requires a sound and consistent methodology fit for purpose, a critical evaluation of assumptions used in the safety assessment calculations, the definition of evolution scenarios utilizing the identification and classification of relevant features, events, and processes (FEPs), a judgement of the impact of FEPs on safety functions, the evaluation of uncertainties, and the interpretation of the calculated results. The methodology of the OPERA safety assessment has been explained in OPERA Deliverable OPERA-PU-NRG2121, "*Report on the safety assessment methodology*" [Grupa, 2014].

The present report describes a reference set of model parameters which are currently applied in the *OPERA Integrated Model* used to perform the OPERA safety assessment calculations. The parameter values applied in the present report are reported as two different sets:

- *Default parameter values*, applied to the conservative or more realistic performance assessment simulations of the *Normal evolution scenario*, utilizing well justified parameter values for five different cases [Grupa, 2017c]:
    - ***Central assessment case (N1):*** all safety functions are assumed to be operating as intended
    - ***Radioactive gas transport case (N2):*** Gas, generated in the repository by processes like corrosion, organic degradation, volatilisation, may potentially drive advective flow and the flow of radioactive gases which are released from the waste packages.
    - ***Gas pressure build-up case (normal expected range, N3):*** In case gas is not able to disperse sufficiently through the engineered barriers or the host rock, a limited build-up of gas pressure may be induced[1].
    - ***Early canister failure case (normal expected range, N4):*** A gradual degradation of steel and concrete in the engineered barrier system (EBS) is part of all *Normal Evolution Scenarios*. However, increased corrosion rates can cause early container failures, e.g. as a result of stress-corrosion cracking[2].
    - ***Deep well assessment case (N5):*** The *Central assessment case* assumes the extraction of groundwater from a moderately deep well [Grupa, 2017c, Section 3.1.3]. The *Deep well assessment case* assumes that drinking water will be

[1] Excessive gas pressure build-up is considered as a separate *What-If case* EGC1, see [Grupa, 2017c, Section 4.9.2]

[2] Excessive early canister failure is addressed as a *What-If case* EEC1, see [Grupa, 2017c, Section 4.9.1].

pumped from larger depths (e.g. 100 - 300 m)[3]. Such activities will short cut a part of the travel path of the radionuclides through the aquifer system.

For the *Normal evolution scenario*, default parameter values are given as well as variants. The default parameter values are denotes as “**DV**”.

- Parameters to be applied in the *uncertainty analyses*.

1.1. Objectives

The main objective of the present report is to collect and summarize parameters relevant to the representation of the five cases of the *Normal Evolution Scenario* in the *OPERA Integrated Model* Additionally, an inventory of parameters has been identified which are specific to a specific future evolution, or scenario, of the OPERA disposal concept.

1.2. Realization

NRG prepared this report, by collecting the relevant input data for use in the ORCHESTRA computer model of the OPERA safety assessment. The parameter selection and classification follows the assessment strategy as defined by the OPERA Safety Case Group (OSCG) in April 2017. According to this strategy, the *Central assessment case* should reflect a best estimate of parameter values related to migration of radionuclides through the Boom Clay, in order to allow a realistic evaluation of the host rock’s performance as main barrier. For the overburden and biosphere, a conservative set of parameter should be selected, in order to address large future uncertainties on the evolution of these compartments.

For the *Central assessment case* (**N1**) of the *Normal evolution scenario*, all required input parameters are reported. *Default values* (DV) of all input parameter are provided, representing justified parameter values for realistic, conservative performance assessment simulation. Furthermore, for several parameters, different set are distinguished in the underlying reports. These parameter values are summarized here as well, organized as *subcases*, additional to the *default values* (an overview of all subcases can be found in Chapter 8). Furthermore, ranges of values as established in the underlying report are summarized here, allow to perform uncertainty analyses. Finally, for the other cases of the *Normal evolution scenario*, the cases **N2** to **N5**, parameter values or model representations that differs from the *Central assessment case* (**N1**) are discussed in a separate Chapter.

1.3. Contents of this Report

This report consists of two data sections. The next five chapters provides input related to the model representation of the *Central assessment case* (**N1**) of the *Normal evolution scenario* and contains default parameter values, parameter values for several subcases and parameter ranges for to the uncertainty analyses:

- Chapter 2 provides an overview of the data relevant for the overall OPERA disposal concept.
- Chapter 3 to 6 provides an overview of the data relevant for the four model compartment *Waste-EBS, Host Rock, Overburden* and *Biosphere*, respectively

Chapter 7 provides data for the other four assessment cases **N2 - N5**. It discusses the specific data which need to be adapted to model these four cases. Some concluding remarks and an overview of all subcases considered are provided in Chapter8.

[3] An extreme case of the *Deep well assessment case* is treated as a part of the *Human Intrusion scenario* – extreme case AH2, see [Grupa, 2017c, Section 4.8].

2. General conceptualization

The model conceptualization is related to the generic, location independent OPERA disposal concept in Boom Clay as described in [Verhoef, 2014a] and further detailed in [Verhoef, 2014b] and [Verhoef, 2015]. Figure 2-1 depicts an artist impression of the OPERA disposal concept and the waste sections that are defined.

Figure 2-1: Artist impression of the OPERA disposal concept (left) and the different disposal sections (right) [Verhoef, 2014a]

2.1.Model compartments overview

In [Verhoef, 2014a], six compartments of the multi-barrier system are distinguished (Figure 2-2).

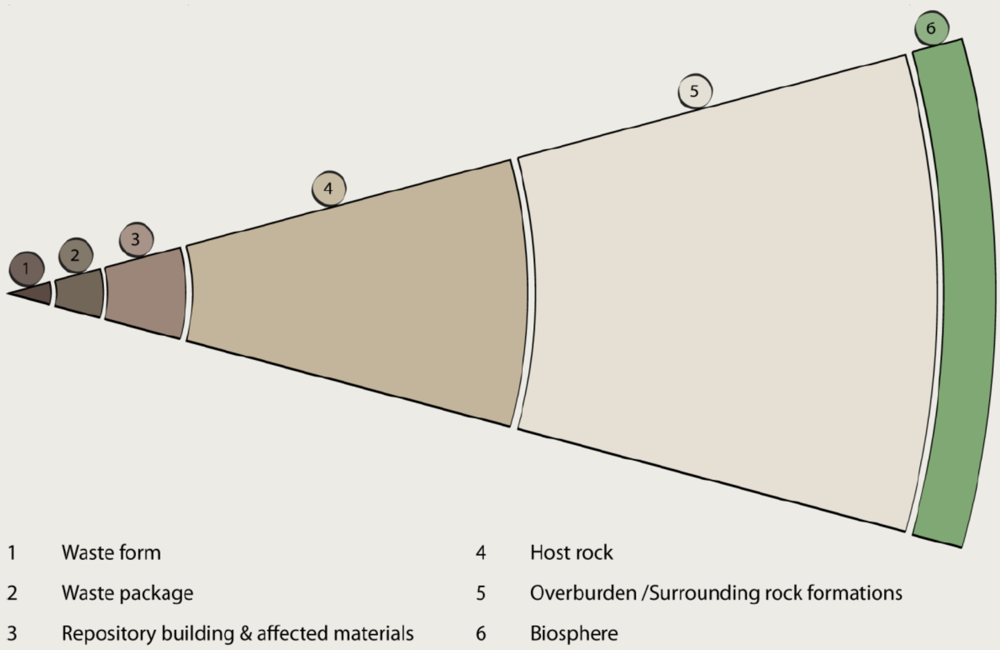

Figure 2-2: Principal compartments of the multi-barrier system [Verhoef, 2014a]

The numerical OPERA performance assessment baseline model is implemented within the ORCHESTRA framework as a 1D-reactive transport model. In the PA model[4] the following *compartments* are defined (Figure 2-3):

1) The *Waste-EBS* compartment, consisting of the *waste form*, the *waste package* and the *repository building & affected materials* (or enclosing *engineered barrier system*);
2) The *Host Rock* (Boom Clay);
3) The *Overburden* (surrounding rock formations);
4) The *Biosphere*.

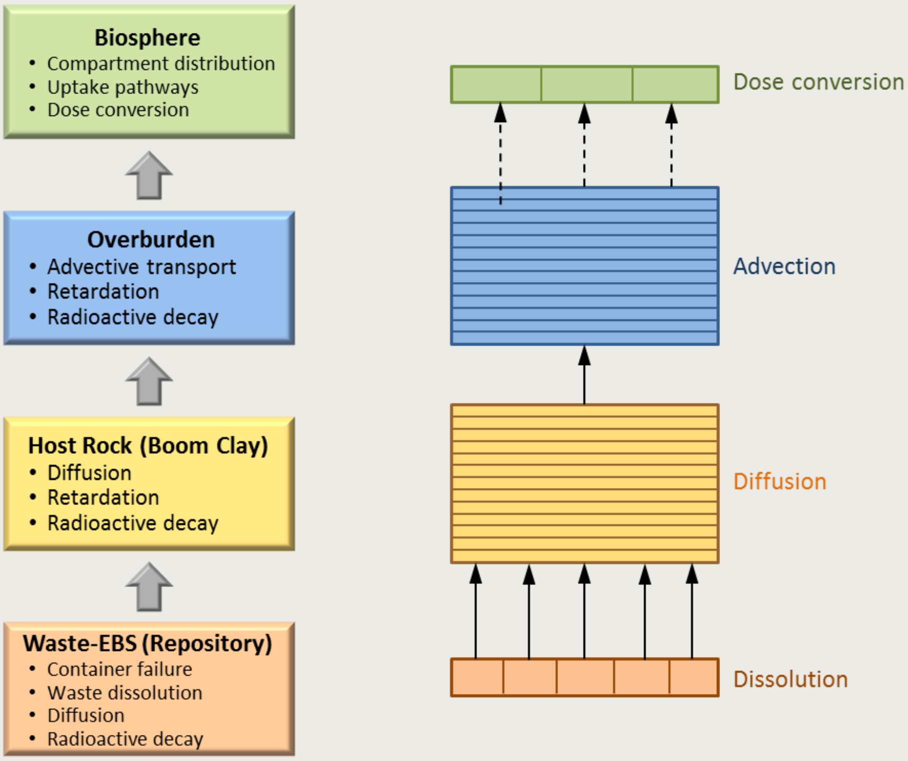

Figure 2-3: Schematic overview of ORCHESTRA PA model compartments

These model compartments are discussed in more detail in the next chapters.

2.2. Radioactive decay

Radioactive decay processes are implemented in each cell of each compartment. The radioactive inventory N_i of a radionuclide i changes in time according to

$$\frac{\partial N_i}{\partial t} = -\lambda_i N_i + \sum_k \gamma_k \cdot \lambda_k N_k \qquad \textbf{Eq. 2-1}$$

with λ_i and λ_k the decay rates of the nuclide i and its mothers k, and γ_k the yield of the reaction. A complete overview of the radionuclides that are accounted for in the long-term post-closure safety assessment is provided in Table 6-1 of [Hart, 2014], and Appendix 1 of [Verhoef, 2015]. Because of the nature of the safety assessment, only radionuclides with half-lives greater than 10 years are taken into account. Shorter living radionuclides are

[4] Status per October 2016

accounted for by including their contribution to risk in the dose conversion factor (see Chapter 6) to the (longer-living) daughter.

Ingrowth of radionuclide decay chains is considered in the safety assessment. The calculation is limited to the longer lived ones, i.e. half-lives longer than 10 years ([Hart, 2014], [Verhoef, 2015]). One exception is one of the last radioactive members of the *4N+1* chain, ^{209}Bi: due to its extremely long half-life (~10^{19} years), it is not taken into account [Verhoef, 2015].

The following simplified actinide decay chains, adapted from [Marivoet; 2012] have been included in the ORCHESTRA PA model:

4N:	^{248}Cm → ^{244}Pu ↘ ^{244}Cm ↗ ^{240}Pu → ^{236}U → ^{232}Th ↘ ^{232}U ↗ stable end member
4N+1:	^{249}Cf → ^{245}Cm → ^{241}Pu → ^{241}Am → ^{237}Np → ^{233}U → ^{229}Th → stable end member
4N+2:	^{246}Cm → ^{242}Pu → ^{238}U ↘ ↑ ^{242m}Am → ^{238}Pu ↗ ^{234}U → ^{230}Th → ^{226}Ra → ^{210}Pb → stable end member
4N+3:	^{247}Cm → ^{243}Am ↘ ↑ ^{243}Cm ↗ ^{239}Pu → ^{235}U → ^{231}Pa → ^{227}Ac → stable end member

The decay rates of all considered radionuclides are derived from the half-lives $T_{½}$ summarized in Table 2-1 according to

$$T_{1/2,i} = \frac{\ln 2}{\lambda_i}$$ **Eq. 2-2**

Table 2-1 give additional information on nuclide decay modes and yields of the four radionuclides chains and their relevant daughters obtained from the OECD/NEA JEFF Database [Kellett, 2009].

Table 2-1: Half-life, prevalent decay mode, yield and relevant daughter of the considered radionuclides of the four nuclide chains [Kellett, 2009].

Nuclide	Half-life $T_{½}$ [a]	Prevalent decay mode	Yield γ [-]	Daughter
^{227}Ac	2.177E+01	*alpha**	*n.a.*	
^{108m}Ag	4.180E+02	*beta*	*n.a.*	
^{241}Am	4.328E+02	*alpha*	1.0000	^{237}Np
^{242m}Am	1.410E+02	*alpha**	0.832	^{238}Pu
			0.168	^{242}Pu
^{243}Am	7.365E+03	*alpha*	1.0000	^{239}Pu
^{133}Ba	1.054E+01	*beta*	*n.a.*	
^{10}Be	1.6E+06	*beta*	*n.a.*	
^{207}Bi	3.176E+01	*beta*	*n.a.*	
^{14}C	5.700E+03	*beta*	*n.a.*	
^{41}Ca	1.03E+05	*beta*	*n.a.*	
^{249}Cf	3.510E+02	*alpha*	1.0000	^{245}Cm
^{36}Cl	3.01E+05	*beta*	*n.a.*	

Nuclide	Half-life $T_{½}$ [a]	Prevalent decay mode	Yield γ [-]	Daughter
^{243}Cm	3.000+01	*alpha*	0.9976	^{239}Pu
			0.0024	^{243}Am
^{244}Cm	1.800E+01	*alpha*	1.0000	^{240}Pu
^{245}Cm	8.500E+03	*alpha*	1.0000	^{241}Pu
^{246}Cm	4.730E+03	*alpha*	0.9997	^{242}Pu
^{247}Cm	1.6E+07	*alpha*	1.0000	^{243}Am
^{248}Cm	3.4E+05	*alpha*	0.9174	^{244}Pu
^{113m}Cd	1.41E+01	*beta*	*n.a.*	
^{135}Cs	2.3E+06	*beta*		
^{137}Cs	3.004E+01	*beta*		
^{152}Eu	1.353E+01	*beta*		
^{3}H	1.233E+01	*beta*		
^{129}I	1.61E+07	*beta*		
^{40}K	1.265E+09	*beta*		
^{81}Kr	2.1E+05	*beta*		
^{85}Kr	1.075E+01	*beta*		
^{93}Mo	4.000E+03	*beta*	0.88	^{93m}Nb
^{93m}Nb	1.613E+01	*IT*	*n.a.*	
^{94}Nb	1.999E+04	*beta*		
^{59}Ni	7.6E+04	*beta*		
^{63}Ni	1.006E+02	*beta*		
^{237}Np	2.140E+06	*alpha*	1.0000	^{233}U
^{231}Pa	3.276E+04	*alpha*	1.0000	^{227}Ac
^{210}Pb	2.216E+01	*alpha**	*n.a.*	
^{107}Pd	6.5E+06	*beta*		
^{145}Pm	1.770E+01	*beta*		
^{238}Pu	8.770E+01	*alpha*	1.0000	^{234}U
^{239}Pu	2.411E+04	*alpha*	1.0000	^{235}U
^{240}Pu	6.563E+03	*alpha*	1.0000	^{236}U
^{241}Pu	1.433E+01	*beta*	1.0000	^{241}Am
^{242}Pu	3.735E+05	*alpha*	1.0000	^{238}U
^{244}Pu	8 E+07	*alpha*	0.9988	^{240}Pu
^{226}Ra	1.600E+03	*alpha*	1.0000	^{210}Pb
^{186m}Re	1.9E+05	*beta**	*n.a.*	
^{79}Se	3.77E+05	*beta*		
^{151}Sm	9.000E+01	*beta*		
^{121m}Sn	5.500E+01	*beta**		
^{126}Sn	2.3E+05	*beta*		
^{90}Sr	2.879E+01	*beta*		
^{99}Tc	2.14E+05	*beta*		
^{229}Th	7.340E+03	*alpha*		
^{230}Th	7.54E+04	*alpha*	1.0000	^{226}Ra
^{232}Th	1.405E+10	*alpha*	*n.a.*	
^{232}U	6.980E+01	*alpha*		
^{233}U	1.593E+05	*alpha*	1.0000	^{229}Th
^{234}U	2.457E+05	*alpha*	0.9984	^{230}Th
^{235}U	7.038E+08	*alpha*	1.0000	^{231}Pa
^{236}U	2.37E+07	*alpha*	1.0000	^{232}Th
^{238}U	4.468E+09	*alpha*	0.9984	^{234}U
^{93}Zr	1.53E+06	*beta*	0.975	^{93m}Nb

* including (shortliving) daughters

3. Compartment *Waste-EBS*

The *Waste-EBS* compartment consists of the waste form, the waste package and the enclosing engineered barrier system (EBS) (Figure 3-1).

Figure 3-1: Artist impression of the waste compartments and the OPERA supercontainer [Verhoef, 2014a].

3.1.General process description

The *Waste-EBS* compartment serves as source term for the risk assessment model. After failure of a waste container (loss of integrity of container, safety function *C1*) at $t_{failure}$, the radionuclide i dissolves slowly from the waste matrix into the volume of the waste package (limitation of contaminated release from waste forms, safety function *R1*). Dissolution takes place at a constant[5] rate λ_{dis}, resulting in a released fraction $X_{i,released}$ of the total waste amount X_i from time $t_{failure}$, until all waste is dissolved[6]:

$$X_{i.released}(t) = \begin{cases} 0 & t \le t_{failure} \\ X_i(t) \cdot \lambda_{dis}(t - t_{failure}) & t_{failure} + 1/\lambda_{dis} \ge t > t_{failure} \\ X_i(t) & t > t_{failure} + 1/\lambda_{dis} \end{cases}$$ **Eq. 3-1**

The released radionuclides are assumed to dissolve in the saturated pore volume (ηV) of the waste package and EBS. This lead after the time $t_{failure}$ to an increase of the dissolved concentration C_i of a radionuclide i in the *Waste-EBS* compartment by waste dissolution. Simultaneously the concentration decreases by diffusion of radionuclides from the *Waste-EBS* compartment into the enclosing *Host Rock* compartment by[6]:

$$\frac{\partial C_i}{\partial t} = \frac{\lambda_{dis}}{\eta V} X_i(t) - D_{pore} \cdot \frac{\partial^2 C_i}{\partial x^2}$$ **Eq. 3-2**

with

C_i concentration nuclide i in solution

D_{pore} pore diffusion coefficient of dissolved nuclide i

After all waste is dissolved, Eq. 3-2 simplifies to

$$\frac{\partial C_i}{\partial t} = -D_{pore} \cdot \frac{\partial^2 C_i}{\partial x^2}$$ **Eq. 3-3**

[5] based on the information available at the moment. If other dissolution behaviours are proposed in WP5.1, the model will be adapted accordingly.

[6] note that although considered (see Eq. 2-1), the terms for radioactive decay and ingrowth are omitted here

In order to exclude in the 1-D model representation diffusion from one disposal section into another, only diffusion out of the *Waste-EBS* to the *Host Rock* is accounted for[7].

3.2. Discretization of Waste-EBS compartment

The *Waste-EBS* compartment is sub-divided into five *disposal sections* (Figure 3-2 and Table 3-1), based on the OPERA waste families described in [Verhoef, 2015]. These waste families groups the radioactive waste from the same origin, of similar nature, and having identical or closely related conditioning characteristics. Each of the disposal sections has its own saturated pore volume ηV, its own container failure time $t_{failure}$ and dissolution rate λ_{dis}.

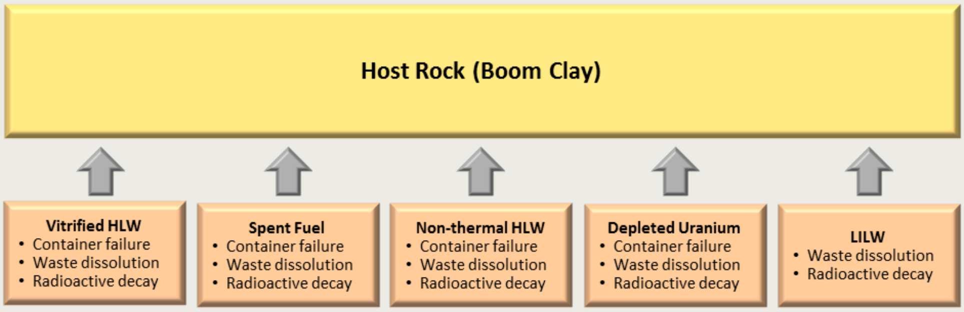

Figure 3-2: Graphical presentation of multiple Waste-EBS compartments

Table 3-1 gives an overview of the five waste sections, the waste allocated there, and the accompanying container and conditioning applied.

Table 3-1: Waste composition of the disposal sections (based on [Verhoef, 2015])

Disposal section	OPERA waste type ("Waste Family")		Waste conditioning	Waste container	Number of waste packages
Vitrified HLW	Vitrified waste (CSD-V)		Vitrified	OPERA supercontainer	478
Spent Fuel	Spent research reactor fuel	HEU	None	OPERA supercontainer	15
		LEU			60
Non-heat-generating HLW	Compacted hulls and ends (CSD-C)		Compacted	OPERA supercontainer	600
	Legacy waste, fissile		Concrete	OPERA supercontainer	100
DepU	Depleted uranium		Concrete	Konrad galvanized steel Type-II container	9060
LILW	Compacted waste		Concrete	200 litre galvanized steel container	140'000
	Processed liquid molybdenum waste		Concrete	1000 litre magnetite container	6000
			Concrete	1000 litre quartz container	2000
	Processed liquid waste with spent ion exchangers		Concrete	1000 litre concrete containers with magnetite aggregate	4000

[7] this is mainly necessary for the calculation of certain performance indicators, see [Rosca-Bocancea, 2016] and [Schröder, 2016]

3.3. Parameter values

3.3.1. Diffusion rate

For the diffusion rate D_{pore} from the *Waste-EBS* compartment to the *Host Rock* compartment (Eq. 3-2 and Eq. 3-3), a conservative value of $3 \cdot 10^{-10}$ m^2/s is assumed, based on [Meeussen, 2017a].

3.3.2. Volumes, footprints, and heights of the waste sections

Based on the information on geometry and properties of the various disposal galleries in [Verhoef, 2014a, 2014b & 2015], saturated porosity volumes ηV and footprint areas A_{waste} have been estimated for the five disposal sections. The estimated porosities for all container types, concrete buffer of the supercontainer, gallery support and backfill material has been summarized in Table 3-2. The volumes of the waste sections refer to the inner side of the excavated Boom Clay, viz. the outer diameter of the gallery lining, and cover only the volumes behind the disposal cell plugs. The results are summarized in Table 3-4. For simplicity, for all waste section an equal height of 2.5 m is assumed (see Eq. 3-2 and Eq. 3-3), i.e. all disposal sections are connected to the *Host Rock* compartment at the same height.

Table 3-2: Estimated porosities for different components of the EBS and waste

component	porosity η [-]	source
backfill	0.45	[Kearsley, 2002]
gallery support	0.15	[Arnold, 2015]
concrete buffer supercontainer	0.15	estimation
ECN canister	0.50	estimation
LILW canister	0.15	[Verhoef, 2014b]
CSD-V canister	0.05	estimation
CSD-C canister	0.20	[Verhoef, 2015]
Konrad type II canister	0.30	estimation

Table 3-3: Overview of the pore volumes and footprint areas of the waste packages and the EBS in the disposal sections (based on [Verhoef, 2014a] and [Verhoef, 2015])

	Pore volume ηV [m^3]			Footprint area A_{waste} [m^2]
Disposal Section	Waste packages	EBS	*Waste-EBS* compartment	EBS
Vitrified HLW	499	1371	1870	3824
Spent Fuel	123	257	380	720
Non-heat-generating HLW	808	1929	2737	5760
DepU	11’829	15’333	27’161	34’790
LILW	6820	39’403	46’222	30’900

3.3.3. Container failure and radionuclide release

Based on the range of uniform corrosion rates as reported in [Kursten, 2014] and an overpack thickness of 34 mm for the OPERA supercontainer [Verhoef, 2014a] it can be calculated that it takes between 15'000 and 6'800'000 years before the overpack is totally corroded. Likewise, for the 3 m thick Konrad type-II container [Verhoef, 2015], periods between 1370 and 2'000'000 years are derived in [Filby, 2016]. However, in [Kursten, 2015] it is noted that "*the high chloride concentrations [...] may result in a significant increased susceptibility to localised corrosion phenomena (such as pitting corrosion, crevice corrosion and stress corrosion cracking*." Besides, it is assumed that failure of a container will occur before it is totally corroded. This results in expert ranges for container failure times 10 times faster than by uniform corrosion only. The resulting upper and lower boundary values are summarized in Table 3-4.

Table 3-4: Estimated ranges for the time of container failure, based on [Kursten, 2015]

	Time of container failure $t_{failure}$ [a]	
	OPERA Supercontainer	**Konrad galvanized steel Type-II container**
Lower boundary	1500	150
Upper boundary	700'000	200'000

Table 3-5 summarizes a range of failure times for the supercontainer to be used for the performance assessment calculations, as suggested in [Neeft, 2017] under the assumption of a pH of 12.5.

Table 3-5: Supercontainer failure times to be used in the *central assessment case* (N1) [Neeft, 2017]

	Time of supercontainer failure $t_{failure}$ [a]
Early container failure case (**EF**)	1000
Failure base case (**DV**)	35'000
Late container failure case (**LF**)	70'000

For the molybdenum waste [Verhoef, 2015], failures times are discussed in [Filby, 2016; Section 5.12]. For all other containers, conservatively an instant failure is assumed. Because in the OPERA performance assessment only five waste sections are distinguished [Verhoef, 2014a], it is conservatively assumed that the molybdenum waste container - as all other container types in the section - fails instantly, too.

Table 3-6 shows the release rates for vitrified waste as derived in [Deissmann, 2016a; Table 6 1]. For all other waste fractions, conservatively instant release is assumed.

Table 3-6: Estimated ranges for the release rates of vitrified waste [Deissmann, 2016a; Table 6-1]

	Vitrified HLW release rate λ_{rel} [1/a]
Lower boundary	$3.8 \cdot 10^{-3}$
Best estimate	$1.5 \cdot 10^{-4}$
Upper boundary	$1.6 \cdot 10^{-7}$

In [Neeft, 2017], for the performance assessment calculations, three cases for the release rate λ_{rel} of the glass matrix of vitrified waste are suggested (Table 3-7).

Table 3-7: Release rates of vitrified waste to be used in the *central assessment case* (N1) [Neeft, 2017]

	Vitrified HLW release rate λ_{rel} [1/a]
Slow release case (**SR**)	$8.9 \cdot 10^{-6}$
Release base case (**DV**)	$5.2 \cdot 10^{-5}$
Fast release case (**FR**)	$3.5 \cdot 10^{-4}$

Table 3-8 summarizes for all waste section of [Verhoef, 2014a] default values for the assumed period $t_{failure}$ after which the containers are assumed to fail, and the release rate λ_{rel}. The values are recommended to be used as default values (**DV**) in the *central assessment case* (**N1**). As part of the *Normal evolution scenario* case **N4**, an early failure of waste packages is assessed as well ($t_{failure}$ = 0; see Chapter 7).

Table 3-8: Overview of WASTE-EBS waste section container failure times and release rates used as default values (DV) for the *central assessment case* (N1), based on [Filby, 2016] and [Neeft, 2017]

Disposal Section	Time of container failure $t_{failure}$ [a]	Release rate λ_{rel} [1/a]
Vitrified HLW	35'000	$5.2 \cdot 10^{-5}$
Spent Fuel	35'000	∞
Non-heat-generating HLW	35'000	∞
DepU	1500	∞
LILW	0	∞

3.3.4. Solubility limit

Solubility limits in the *Waste-EBS* compartment are defined for three elements: *U*, *Th*, and *Np*. Table 3-9 summarizes the values derived in [Schröder, 2017c]

Table 3-9: Best estimate solubility values in the *Waste-EBS* compartment (DV).

Element	Solubility limit S [mol/l]
U	$1.0 \cdot 10^{-5}$
Th	$1.0 \cdot 10^{-5}$
Np	$1.0 \cdot 10^{-3}$

The solubility of uranium is expected to influence strongly the risk at very long terms. To address the large uncertainty discussed in [Schröder, 2017c], next to the best estimate (DV) in Table 3-9, a low solubility case (LS) is defined (Table 3-10). The solubility of *Th* and *Np* are expected to be of less relevance, no alternative cases are defined here.

Table 3-10: Recommend solubilities of uranium for the central assessment case (N1)

Cases	Solubility limit S [mol/l]
Solubility base case (**DV**)	$1 \cdot 10^{-5}$ mol/l
Low solubility case (**LS**)	$1 \cdot 10^{-6}$ mol/l

3.3.5. Radionuclide inventories

The inventories of the radionuclides in the various types of radioactive waste at the time of disposal (foreseen in 2130) have been reported in [Hart, 2014] and [Verhoef, 2015]. The radionuclide inventories for the different *WASTE-EBS* compartments are given in Table 3-11 and are based on the inventory and number of waste packages given in [Verhoef, 2015; Figure 2-1 and Appendix 1]. The radionuclide inventories of radionuclides have been obtained by multiplying the number of waste packages [Verhoef, 2015; Figure 2-1] with the activities reported in the tables of Appendix 1 of [Verhoef, 2015]:

- *Vitrified HLW:* Table A-2
- *Spent Fuel (HEU+LEU):* Table A-4
- *Non-heat-generating HLW*:
  - *Compacted hulls and ends:* Table A-2
  - *Legacy waste:* Table A-5
- *Depleted uranium:* Table A-7
- *LILW:*
  - *Compacted waste:* Table A-7
  - *Processed liquid molybdenum waste (magnetite container)*: Table A-6
  - *Processed liquid molybdenum waste (quartz container):* Table A-6
  - *Processed liquid waste with spent ion exchangers*: Table A-7

Table 3-11: Inventory of disposal sections ([Verhoef, 2015])

Nuclide	Half-life [a]	Inventory of disposal sections [Bq]				
		Vitrified HLW	Spent Fuel	Non-heat-generating HLW	DepU	LILW
^{227}Ac	2.177E+01	2.901E+05	-	-	-	1.834E+07
^{108m}Ag	4.180E+02	-	-	9.909E+05	-	1.304E+12
^{241}Am	4.328E+02	5.067E+16	1.687E+15	3.247E+13	-	2.100E+13
^{242m}Am	1.410E+02	7.457E+10	-	9.360E+10	-	-
^{243}Am	7.365E+03	1.228E+15	4.313E+12	3.690E+11	-	6.353E+09
^{133}Ba	1.054E+01	-	-	-	-	2.548E+06
^{10}Be	1.6E+06	-	-	-	-	2.826E+09
^{207}Bi	3.176E+01	-	-	-	-	4.774E+07
^{14}C	5.700E+03	-	9.855E+09	8.389E+12	-	3.113E+13
^{41}Ca	1.03E+05	-	-	1.793E+09	-	8.000E+09
^{249}Cf	3.510E+02	-	-	1.962E+06	-	1.848E+07
^{36}Cl	3.01E+05	-	-	-	-	2.234E+10
^{243}Cm	3.000E+01	6.07E+13	1.56E+14	7.76E+11	-	3.66E+11
^{244}Cm	1.800E+01	1.056E+15	2.386E+12	8.292E+12	-	7.586E+09
^{245}Cm	8.500E+03	1.386E+12	1.820E+10	6.629E+09	-	4.264E+07
^{246}Cm	4.730E+03	2.280E+13	2.276E+09	2.873E+09	-	5.354E+06
^{247}Cm	1.6E+07	1.257E+08	3.235E+08	1.610E+06	-	7.592E+05
^{248}Cm	3.4E+05	7.744E+08	1.993E+09	9.937E+06	-	4.952E+06
^{113m}Cd	1.41E+01	-	-	-	-	-
^{135}Cs	2.3E+06	1.439E+13	2.561E+12	6.322E+11	-	8.160E+10
^{137}Cs	3.004E+01	1.577E+17	9.153E+15	2.066E+15	-	4.654E+14
^{152}Eu	1.353E+01	-	-	2.353E+09	-	3.497E+07
^{3}H	1.233E+01	-	-	1.502E+13	-	1.512E+12
^{129}I	1.61E+07	-	3.948E+10	3.304E+10	-	3.629E+09
^{40}K	1.265E+09	-	-	-	-	5.908E+09
^{81}Kr	2.1E+05	-	-	-	-	3.976E+06
^{85}Kr	1.075E+01	-	7.926E+12	7.240E+11	-	1.904E+09
^{93}Mo	4.000E+03	-	-	3.520E+12	-	1.564E+09
^{93m}Nb	1.613E+01	-	-	-	-	1.484E+04
^{94}Nb	1.999E+04	-	2.010E+08	3.374E+13	-	1.914E+11
^{59}Ni	7.6E+04	-	-	2.182E+14	-	1.758E+12
^{63}Ni	1.006E+02	-	1.059E+06	1.058E+16	-	9.598E+14
^{237}Np	2.140E+06	2.294E+13	5.916E+11	2.142E+10	-	8.214E+07
^{231}Pa	3.276E+04	-	2.115E+08	-	-	5.574E+07
^{210}Pb	2.216E+01	-	-	-	-	1.079E+09
^{107}Pd	6.5E+06	3.241E+12	1.944E+10	4.676E+09	-	3.297E+08
^{145}Pm	1.770E+01	-	-	-	-	9.260E+01
^{238}Pu	8.770E+01	2.285E+14	1.139E+15	7.500E+14	-	9.675E+12
^{239}Pu	2.411E+04	6.883E+13	1.899E+14	1.290E+14	-	1.824E+12
^{240}Pu	6.563E+03	1.104E+14	1.784E+14	2.212E+14	-	1.161E+11
^{241}Pu	1.433E+01	3.513E+13	1.154E+14	8.502E+13	-	6.567E+08
^{242}Pu	3.735E+05	4.828E+11	6.449E+11	1.256E+12	-	2.786E+11
^{244}Pu	8E+07	2.347E+08	6.039E+08	3.009E+06	-	-
^{226}Ra	1.600E+03	4.923E+04	1.317E+08	5.320E+06	-	9.366E+11
^{186m}Re	1.9E+05	-	-	-	-	3.318E+09
^{79}Se	3.77E+05	9.608E+12	2.026E+11	5.100E+10	-	1.281E+10
^{151}Sm	9.000E+01	2.615E+16	1.328E+15	3.269E+14	-	2.166E+12
^{121m}Sn	5.500E+01	-	-	-	-	7.994E+09
^{126}Sn	2.3E+05	1.816E+13	2.288E+13	6.856E+10	-	2.851E+10
^{90}Sr	2.879E+01	9.799E+16	7.512E+15	1.886E+15	-	1.958E+14
^{99}Tc	2.14E+05	5.975E+14	1.665E+13	2.230E+13	-	1.483E+11
^{229}Th	7.340E+03	5.593E+06	1.965E+06	7.990E+04	-	3.150E+07
^{230}Th	7.54E+04	8.030E+07	4.830E+09	1.954E+08	-	3.976E+06
^{232}Th	1.405E+10	-	-	-	-	-

Nuclide	Half-life [a]	Inventory of disposal sections [Bq]				
		Vitrified HLW	Spent Fuel	Non-heat-generating HLW	DepU	LILW
^{232}U	6.980E+01	1.410E+12	3.629E+12	1.804E+10	4.240E+12	2.366E+07
^{233}U	1.593E+05	1.530E+09	2.745E+08	1.127E+07	-	2.857E+08
^{234}U	2.457E+05	2.280E+11	5.991E+12	1.724E+11	1.567E+15	7.213E+10
^{235}U	7.038E+08	1.377E+09	7.800E+10	3.610E+09	3.135E+13	1.927E+11
^{236}U	2.37E+07	2.012E+10	9.288E+11	3.026E+10	3.715E+14	1.338E+09
^{238}U	4.468E+09	2.643E+10	1.130E+11	1.134E+10	1.359E+15	5.362E+12
^{93}Zr	1.53E+06	5.019E+13	2.505E+12	5.416E+12	-	6.438E+09

An analysis on different energy scenarios has been performed in [Hart, 2016], and some uncertainty ranges on waste fractions are discussed in [Hart, 2014]. However, both are not part of the OPERA assessment [Verhoef, 2011 & 2014s] and are thus not elaborated here in more detail.

4. Compartment Host Rock

4.1. General process description

In Boom Clay, the radionuclides are migrating slowly from the waste sections to the surrounding aquifers by diffusion (safety function *R3*). Advective transport by mass flow of the solute is assumed insignificant under normal evolution (safety function *R2*) and is thus not considered in the *Normal evolution scenario*.

The transport rate of radionuclides, once released from the waste packages, through the Boom Clay host rock depends on the following processes:

- The solubility of the radionuclide in the Boom clay
- The distribution of radionuclides over the solid and solution phase, and
- the diffusion of nuclides in solution through the Boom Clay;

Diffusion takes place in the solution phase only. Two fractions of radionuclides are distinguished for computing migration: free radionuclide species in the aqueous phase, $C_{i,aq}$, and radionuclides bound to dissolved organic matter (DOC), $C_{i,DOC}$. Both fractions have different diffusion rates, and are therefore addressed separately. Assuming a 1D-model representation to be sufficient for the considered disposal facility, the overall diffusive transport of a radionuclide i can be computed by considering both fractions[8]:

$$\frac{\partial C_{i,aq}}{\partial t} = \frac{D_{i,aq}}{R_{i,aq}} \cdot \frac{\partial^2 C_{i,aq}}{\partial x^2}$$ **Eq. 4-1**

and

$$\frac{\partial C_{i,DOC}}{\partial t} = \frac{D_{DOC}}{R_{i,DOC}} \cdot \frac{\partial^2 C_{i,DOC}}{\partial x^2}$$ **Eq. 4-2**

with

$C_{i,aq}$	aqueous concentration of the free ions of nuclide i
$C_{i,DOC}$	DOC-bound concentration of nuclide i
$D_{i,aq}$	pore diffusion coefficient of dissolved nuclide i
D_{DOC}	pore diffusion coefficient of DOC
$R_{i,aq}$	retardation factor of nuclide i dissolved in the aqueous phase[-],
$R_{i,DOC}$	retardation factor of DOC-bound nuclide i [-],

The mathematical models to describe diffusive transport in porous media are outlined in [Meeussen, 2017a; Section 6.1], and the approach to derive retardation factors and the related K_d-values is described in [Schröder, 2017b]. The retardation factor R_i of a radionuclide i as used in the transport model (Eq. 4-1) can be derived from the K_d-values and related bulk matrix density ρ and porosity η according to:

$$R_{i,aq} = 1 + \frac{\rho}{\eta} K_{d_{i,aq}}$$ **Eq. 4-3**

and

$$R_{i,DOC} = 1 + \frac{\rho}{\eta} K_{d_{i,DOC}}$$ **Eq. 4-4**

Influx from the *Waste-EBS* model component is calculated by diffusion.

[8] note that although considered (see Eq. 2-1), the terms for radioactive decay and ingrowth are omitted here

4.2. Discretization of Host Rock compartment

In the present OPERA safety assessment model the Boom Clay (compartment *Host Rock*) is conceptualized as a pseudo-2D model consisting of 50 cells. The model represents only upwards diffusion to the surface, diffusion deeper into the clay (and consequently into the *Overburden*) is assumed to be identical to the upwards diffusion, i.e. only the upper half is represented by the model, while the lower half is mirrored by a no-flux boundary (Neumann boundary condition). The pseudo-2D model representation makes use of cells with variable cell volumes and contact areas (Table 4-1, see [Meeussen, 2017]).

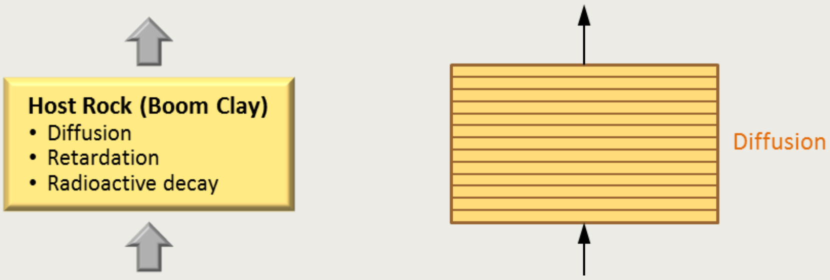

Figure 4-1: Conceptualization of the Boom Clay

An overview of the general parameters required as input for the Boom Clay compartment is given in Table 4-2. The porosity and other more specific parameters related to the transport of radionuclides are mentioned in the following sections.

Table 4-1: Cell dimensions of the "pseudo" 2D model for the OPERA safety assessment

cellnr	cellvolume [l]	distance to centre [m]	contact area [m^2]
1	1000	0.65	2
2	3000	0.65	4
3	5000	0.65	6
4	7000	0.65	8
5	9000	0.65	10
6	11000	0.65	12
7	13000	0.65	14
8	15000	0.65	16
9	17000	0.65	18
10	19000	0.65	20
11	21000	0.65	22
12	23000	0.65	24
13	25000	0.65	26
14	27000	0.65	28
15	29000	0.65	30
16	31000	0.65	32
17	33000	0.65	34
18	35000	0.65	36
19	37000	0.65	38
20	39000	0.65	40
21	41000	0.65	42
22	43000	0.65	44
23	45000	0.65	46
24	47000	0.65	48
25	49000	0.65	50
26-50	25000	0.5	25

Table 4-2: General Boom Clay geometrical parameters required for the OPERA safety assessment

Parameter	Value	Unit	Source
Diffusion distance x	47.5	[m]	[Verhoef 2014a]
Number of cells	50	[-]	
Cell heights H_{BC}	0.5 - 1.0	[m]	see Table 4-2
area $A_{host\ rock}$	76'000	[m^2]	see Table 3-3

4.3. Parameter values

4.3.1. Solubility limit

Solubility limits in the *Host Rock* compartment are defined for two elements: *U* and *Np*. **Table 4-3** summarizes the values evaluated in [Schröder, 2017c].

Table 4-3: Best estimate solubility values in the *Host Rock* compartment.

Element	Case	Solubility limit S [mol/l]
U		$1.0 \cdot 10^{-4}$
Np	base case (**DV**)	$2.1 \cdot 10^{-5}$
	low DOC case (LD)	$4.2 \cdot 10^{-6}$
	high DOC case (HD)	$4.2 \cdot 10^{-5}$

4.3.1. Sorption parameter

Nuclide-specific retardation values as input for Eq. 4-1 are determined in [Schröder, 2017b]. The values are derived by detailed geochemical calculation implemented in ORCHESTRA and reflect the variability of geochemical properties as expected in the Netherlands (Table 4-4). The used methods, data and assumptions are documented in [Schröder, 2017a & 2017b].

Because no relevant data on DOC concentrations in Boom Clay of the Netherlands was available, a conservative, large range of DOC concentrations was established, covering low concentrations as measured in the Netherlands *above* the Boom Clay [Griffioen, 2015] as expected under saline conditions, and the higher concentrations as found in Mol. Three subcases are defined in order to avoid too large ranges that are probably not valid on any single location:

- a ***base case*** (**DV**) with a DOC concentration of 100 mg/l,
- a ***low DOC case*** (**LD**) with a DOC concentration of 20 mg/l, and
- a ***high DOC case*** (**HD**) with a DOC concentration of 200 mg/l.

Correspondingly, three sets of calculations were carried out and for each of these subcases upper, central and lower R-values were computed. The resulting ranges are summarized in Table 4-5 for the *base case*. Table 4-6 provides central R-values (**DV**) for the *base case*, and Appendix 2 contains additional values for the other two subcases.

Table 4-4: Ranges of Boom Clay properties used for the derivation of ranges of K_d-values in [Schröder, 2017b]

Parameter	Range
Bulk wet density [kg/m3]	*1.900 – 2.150*
Porosity [%]	*29 – 43*
CEC Boom Clay [meq/100g Boom Clay]	*2.0 – 42*
SOC [wt. %]	*0.35 – 2.0*
Proton exchange capacity SHA [meq/g]	*1 – 2*
DOC [mg/L]	***base case:** 100 mg/l* ***low DOC case**: 20 mg/l* ***high DOC case:** 200 mg/l*
Proton exchange capacity DHA [meq/g]	*2 – 6*
HFO [g/kg]	*0.4 – 3.3*
Inorganic carbon [wt. %]	*0.0 – 2.5*
Total amount Ca [wt. %]	*0.2 – 7.3*
Total amount Fe [wt. %]	*2.2 – 5.4*
Total amount S [wt. %]	*0.35 – 2.6*
Soluble concentration Cl [mg/L]	*4 – 20'000*
Soluble concentration Na [mg/L]	*4 – 11'000*
pH [-]	*7.7 – 9.2*
pe + pH [-]	*3.8 – 5.8*

Table 4-5: Lower and upper R-values for dissolved and DOC-bound fractions of the radionuclides considered in OPERA (base case, 100 mg/l DOC) [Schröder, 2017a]

Group	Element	Retardation factor R_{aq} [-]			Retardation factor R_{DOC} [-]		
		Lower value	Mean value	Upper value	Lower value	Mean value	Upper value
conservatively set to one	H	1			>50'000		
	C						
	Si						
	Cl						
	Ar						
	Ti						
	Kr						
	Mo						
	Nb						
	Ba						
	Pm						
	Ho						
	Re						
	Bi						
	Po						
based on model calculations	K	3	34	1997	525	2300	5694
	Ni	>50'000			81	227	494
	Sn				77	221	489
	Cd				78	222	490
	Pb				120	338	1145
based on model calculations, experimental support from Boom Clay (Mol)	I	1			>50'000		
	Se	1			>50'000		
	Ca	46	5409	>50'000	611	2881	9584
	Sr	160	13329	>50'000	161	461	1375
	Tc	>50'000			77	221	489
	Cs	476	6454	38699	16611	>50'000	>50'000
	Ra	87	7320	>50'000	161	458	1364
	Th	>50'000			77	221	489
	U	33	>50'000	>50'000	77	221	489
	Eu	>50'000			95	267	706
	Np				77	221	489
	Pu				77	221	489
	Am				116	349	1676
	Cm				78	222	489
extrapolated on basis of chemical similarities	Be	46	5409	>50'000	611	2881	9584
	Zr	>50'000			77	221	489
	Pd				77	221	489
	Ag				77	221	489
	Sm				77	221	489
	Ac				77	221	489
	Pa	33	>50'000	>50'000	77	221	489
	Cf	33	>50'000	>50'000	77	221	489

Table 4-6: Default R-values (DV) for dissolved and DOC-bound fractions of the radionuclides considered in OPERA for the *central assessment case* N1 (base case, 100 mg/l DOC) [Schröder, 2017a]

Element	Retardation factor R_{aq} [-]	Retardation factor R_{DOC} [-]
H	1	50000
Be	5409	2881
C	1	50000
Cl	1	50000
K	34	2300
Ca	5409	2881
Ni	50000	227
Se	1	621
Kr	1	50000
Sr	13329	461
Mo	1	50000
Nb	1	50000
Zr	50000	221
Tc	50000	221
Pd	50000	221
Ag	50000	221
Cd	50000	222
Sn	50000	221
I	1	50000
Ba	1	50000
Cs	6457	50000
Pm	1	50000
Sm	50000	221
Eu	50000	267
Re	1	50000
Pb	50000	338
Bi	1	50000
Ra	7320	458
Ac	50000	221
Th	50000	221
Pa	50000	221
Np	50000	221
U	50000	221
Pu	50000	221
Am	50000	349
Cm	50000	222
Cf	50000	221

4.3.1. Diffusion parameter

Nuclide-specific diffusion properties as input for Eq. 4-1 are determined in [Meeussen, 2017b]. The resulting ranges are summarized in Table 4-7 (diffusion properties of radionuclides) and Table 4-8 (diffusion properties of DOC). The values are derived by detailed geochemical calculation implemented in ORCHESTRA and reflect the variability of geochemical properties as expected in the Netherlands. The used methods, data and assumptions are documented in [Meeussen, 2017a; Chapters 3 to 5]. Table 4-9 and Table 4-10 provide default values (**DV**) to be used in the *central assessment case* **N1**.

Table 4-7: Ranges of diffusion properties for the elements considered in OPERA [Meeussen, 2017b, Table 2-1]. For Se, the most conservative values for (Se(I)) are taken.

Element	*Diffusion accessible porosity η [-]*		*Pore diffusion coefficient D_{pore} [m^2s^{-1}]*	
	min	max	min	max
H	0.14	0.40	$2.0\cdot10^{-10}$	$2.6\cdot10^{-10}$
Be	0.07	0.17	$2.0\cdot10^{-10}$	$2.0\cdot10^{-09}$
C	0.05	0.40	$1.5\cdot10^{-11}$	$1.0\cdot10^{-10}$
Cl	0.05	0.40	$1.0\cdot10^{-10}$	$1.6\cdot10^{-10}$
K	0.14	0.40	$1.4\cdot10^{-10}$	$8.1\cdot10^{-09}$
Ca	0.14	0.40	$1.9\cdot10^{-10}$	$3.3\cdot10^{-10}$
Ni	0.07	0.17	*n.a.*	*n.a.*
Se	0.05	0.40	$8.4\cdot10^{-11}$	$1.3\cdot10^{-10}$
Kr	0.14	0.40	$2.0\cdot10^{-10}$	$2.6\cdot10^{-10}$
Sr	0.14	0.40	$1.9\cdot10^{-10}$	$3.3\cdot10^{-10}$
Mo	0.05	0.40	$5.0\cdot10^{-11}$	$8.0\cdot10^{-11}$
Nb	0.05	0.40	$6.7\cdot10^{-11}$	$1.1\cdot10^{-10}$
Zr	0.07	0.17	*n.a.*	*n.a.*
Tc	0.07	0.17	*n.a.*	*n.a.*
Pd	0.07	0.17	*n.a.*	*n.a.*
Ag	0.07	0.17	*n.a.*	*n.a.*
Cd	0.07	0.17	*n.a.*	*n.a.*
Sn	0.07	0.17	*n.a.*	*n.a.*
I	0.05	0.40	$1.0\cdot10^{-10}$	$1.6\cdot10^{-10}$
Ba	0.14	0.40	$1.9\cdot10^{-10}$	$3.3\cdot10^{-10}$
Cs	0.14	0.40	$1.4\cdot10^{-10}$	$8.5\cdot10^{-09}$
Pm	0.07	0.17	$2.0\cdot10^{-10}$	$2.0\cdot10^{-09}$
Sm	0.07	0.17	*n.a.*	*n.a.*
Eu	0.07	0.17	*n.a.*	*n.a.*
Re	0.05	0.40	$5.7\cdot10^{-12}$	$8.5\cdot10^{-09}$
Pb	0.07	0.17	*n.a.*	*n.a.*
Bi	0.05	0.40	$5.7\cdot10^{-12}$	$8.5\cdot10^{-09}$
Ra	0.14	0.40	$1.8\cdot10^{-10}$	$3.1\cdot10^{-10}$
Ac	0.07	0.17	*n.a.*	*n.a.*
Th	0.07	0.17	*n.a.*	*n.a.*
Pa	0.07	0.17	$2.0\cdot10^{-10}$	$2.0\cdot10^{-09}$
Np	0.07	0.17	*n.a.*	*n.a.*
U	0.07	0.17	$2.0\cdot10^{-10}$	$2.0\cdot10^{-09}$
Pu	0.07	0.17	*n.a.*	*n.a.*
Am	0.07	0.17	*n.a.*	*n.a.*
Cm	0.07	0.17	*n.a.*	*n.a.*
Cf	0.07	0.17	$2.0\cdot10^{-10}$	$2.0\cdot10^{-09}$

Table 4-8: Ranges of diffusion properties for DOC [Meeussen, 2017a, Table 6-9]

Diffusion accessible porosity η_{DOC} [-]		Pore diffusion coefficient D_{pore} [m^2s^{-1}]	
min	max	min	max
0.07	0.17	$5.7\cdot10^{-12}$	$5.7\cdot10^{-11}$

Table 4-9: Default values (DV) with diffusion properties for the elements considered in OPERA for the *central assessment case* N1 [Meeussen, 2017b, Table 2-1]. For Se, the most conservative values for (Se(l)) are taken.

Element	*Diffusion accessible porosity η [-]*	*Pore diffusion coefficient D_{pore} [m^2s^{-1}]*
H	0.27	$2.3 \cdot 10^{-10}$
Be	0.12	$6.0 \cdot 10^{-10}$
C	0.23	$3.9 \cdot 10^{-11}$
Cl	0.23	$1.3 \cdot 10^{-10}$
K	0.27	$1.1 \cdot 10^{-09}$
Ca	0.27	$2.5 \cdot 10^{-10}$
Ni	0.12	*n.a.*
Se	0.23	$1.0 \cdot 10^{-10}$
Kr	0.27	$2.3 \cdot 10^{-10}$
Sr	0.27	$2.5 \cdot 10^{-10}$
Mo	0.23	$6.3 \cdot 10^{-11}$
Nb	0.23	$8.6 \cdot 10^{-11}$
Zr	0.12	*n.a.*
Tc	0.12	*n.a.*
Pd	0.12	*n.a.*
Ag	0.12	*n.a.*
Cd	0.12	*n.a.*
Sn	0.12	*n.a.*
I	0.23	$1.3 \cdot 10^{-10}$
Ba	0.27	$2.5 \cdot 10^{-10}$
Cs	0.27	$1.1 \cdot 10^{-09}$
Pm	0.12	$6.0 \cdot 10^{-10}$
Sm	0.12	*n.a.*
Eu	0.12	*n.a.*
Re	0.23	$2.2 \cdot 10^{-10}$
Pb	0.12	*n.a.*
Bi	0.23	$2.2 \cdot 10^{-10}$
Ra	0.27	$2.4 \cdot 10^{-10}$
Ac	0.12	*n.a.*
Th	0.12	*n.a.*
Pa	0.12	$6.0 \cdot 10^{-10}$
Np	0.12	*n.a.*
U	0.12	$5.48 \cdot 10^{-10}$
Pu	0.12	*n.a.*
Am	0.12	*n.a.*
Cm	0.12	*n.a.*
Cf	0.12	$6.0 \cdot 10^{-10}$

Table 4-10: Default values (DV) of diffusion properties for DOC for the *central assessment case* N1 [Meeussen, 2017a, Table 6-9]

Diffusion accessible porosity η_{DOC} [-]	Pore diffusion coefficient D_{pore} [m^2s^{-1}]
0.12	$1.8 \cdot 10^{-11}$

5. Compartment *Overburden*

5.1. *General process description*

In the overburden, the radionuclides are migrating slowly from the Boom Clay to the biosphere by advective transport and diffusion (safety function *R3*). Under normal evolution (safety function *R2*), advective transport is limited to the soluble phase: mass transport in the gas phase is thus not considered in the Central assessment case N1 (see also the cases N2 and N3, Chapter 7).

The overall diffusive/advective transport of a radionuclide i is calculated by a 1D transport equation[9]:

$$\frac{\partial C_i}{\partial t} = -\frac{v}{R_i}\frac{\partial C_i}{\partial t}$$ **Eq. 5-1**

with v the effective flow velocity. The influx of radionuclides from the Boom Clay model compartment into the overburden model is calculated by diffusion, with the flow velocity v perpendicular on the diffusive flow (Figure 5-1):

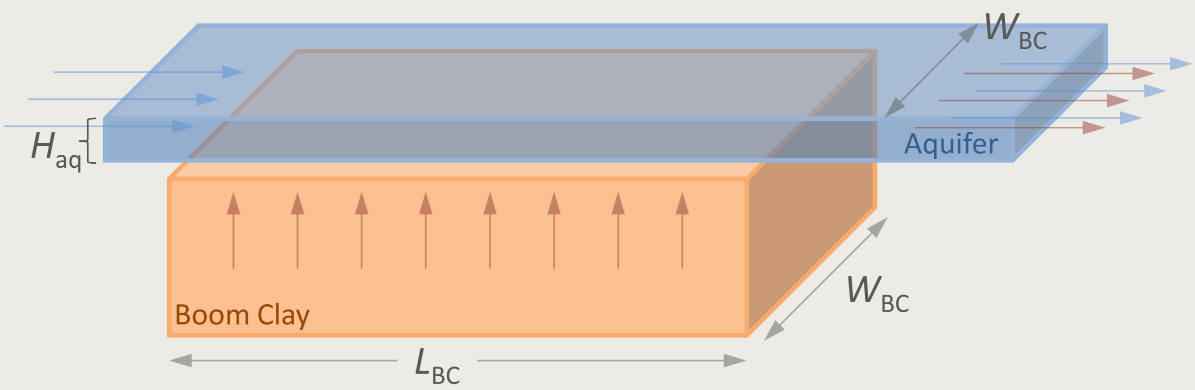

Figure 5-1: Schematic of RN transfer at *Host Rock* - *Overburden* interface

The influx J_i of a radionuclide i is calculated according to

$$J_i = D_{pore,i}\frac{\partial C_i}{\partial x_{\text{int}}}$$ **Eq. 5-2**

with x_{int} the distance between the compartments [Grupa, 2017b]. The diffusion distance x_{int} can be derived by the center-to-center distance of the interface cells

$$x_{\text{int}} = \frac{H_{BC} + H_{aq}}{2}$$ **Eq. 5-3**

with H_{BC} the height of the top *Host Rock* cell (Table 4-2), and H_{aq} the variable height of the Overburden cells (see next section).

[9] note that although considered (see Eq. 2-1), the terms for radioactive decay and ingrowth are omitted here

The concentration $C_{i,ov}$ of a radionuclide i in the *Overburden* decreases during the transport along the pathline due to vertical dispersion of the plume. In the OPERA safety assessment model, dispersion is represented in a simplified manner by applying a dispersion dilution factor F_{disp} to the *Overburden* cell *Ov_last* that interfaces with one of the *Biosphere* compartments, according to:

$$C_{i,Ov\_last} = \frac{C_{i,Ov\_first}}{F_{disp}} \quad \text{Eq. 5-4}$$

with C_{i,ov_first} the concentration of radionuclide i in one of the previous *Overburden* cells.

5.2. Discretization of the Overburden compartment

In the present OPERA safety assessment model the aquifer is conceptualized as a single compartment consisting of 50 cells connected by an “advection” link (see Figure 5-2). The flow path of the hydrological component starts of at the top of the Boom Clay layer and ends in three different pathways to the *Biosphere* compartment. The length of each of the cells is determined by the total length of the flow path from the top of the Boom Clay to the biosphere divided by 50.

A width of the flow path of 1100 m is assumed, representing the smaller dimension of the disposal facility (Figure 2-1, [Verhoef, 2014a]). The height of the *Overburden* compartment is chosen in a way that it allow a conservative 1D-model representation with a constant interface area between the *Overburden* model cells. The vertical spread of the plume by dispersion is accounted for by applying a *dispersion dilution factor* F_{disp}: the *dispersion dilution factor* represents the dilution of the plume over the whole length by vertical dispersion and is applied at the end of the pathline to the last cell of the *Overburden* compartment that connects to the Biosphere.

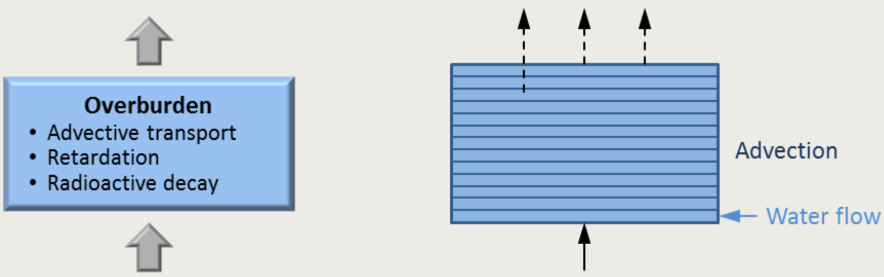

Figure 5-2: Schematic representation of the hydrological transport component

An overview of the geometrical and general parameters required in ORCHESTRA as input for the compartment *Overburden* is given in Table 5-1. Other geometric properties can vary and are discussed in the next section.

Table 5-1: General parameters of the *Overburden* compartment required for the OPERA safety assessment

Parameter	Value	Unit	Source
Path length x	14’000 -28’200	[m]	[Valstar, 2016a]
Number of cells	50		
Width w	1100	[m]	[Verhoef, 2014a], see text
Cell length	280 - 564	[m]	[Valstar, 2016a],

5.3. Parameter values

5.3.1. Travel time and general hydrological parameters

The groundwater flow is conceptualized by an effective velocity representing the hydraulic transport models developed in Task 6.2.1. The effective groundwater velocity is related to the initial flow rate in the *Overburden* obtained from detailed hydraulic calculations carried out within Task 6.2.1. The initial flow rate is not directly linked to the traveltime, but correlated to the dilution by dispersion. The effective groundwater velocity (or initial flow rate) is therefore discussed in Section 5.3.2.

The results are provided in Table 5-2, containing data on the total travel distances and corresponding residence times, averaged porosities and effective flow velocities for three subcases: ***fast*** (**DV**), ***medium*** (**MS**) and ***slow*** (**SS**) streamlines, representing respectively the 10-, 50-, and 90-percentile of the calculated residence times [Valstar, 2017; Section 3.3]. The lowest residence time found in [Valstar, 2017, Figure 3.5] is about 1000 years, and it is noted that in general the values given "*should be considered as a first, order of magnitude, estimate for conservative travel times only*" [Valstar, 2017, Section 6.1]. [Valstar, 2017] derived for the different streamlines values for the *equivalent height* H_{aq} between 2.6 and 3.9 m (Table 5-2).

Table 5-2: Travel distances, averaged porosities, travel times, flow velocities, and cell heights at the interface *Host Rock - Overburden* [Valstar, 2017] for the three subcases of fast, medium and slow streamlines, for a moderate climate (DV)

Streamline	Path length x [km]	Porosity η_{aq} [-]	Travel time [yr]	Equivalent height H_{aq} [m]	Cell height x_{int} [-]
Fast (**DV**)	23.3	0.38	30'700	2.84	1.92
Medium (**MS**)	14.0	0.28	164'000	3.86	2.43
Slow (**SS**)	28.2	0.30	853'000	2.67	1.84

Future hydraulic boundary conditions in the Boom Clay and geohydrological scenarios have been described in [Ten Veen, 2015; Chapter 3]. The uncertainty with respect to the geohydrology for future geological scenarios was considered in the hydraulic calculations in [Valstar, 2017; Section 4.2] and represented there in the form of *maximum reduction factors* of the total travel times, for four climatic subcases as given in Table 5-3. However, a closer examination shows that the reduction factor does not apply equally to all travel times. In ([Valstar, 2017], the minimum and 10-percentile of the residence time was estimated, and is summarized in Table 5-3.

Table 5-3: Maximum reduction factor of the total travel time, minimum value and 10-percentiel of the travel time for the different climate conditions [Valstar, 2017]

Climate subcase	Maximum reduction factor of the total travel time [-]	Travel times: Minimum value [yr]	Travel times: 10-percentile [yrs]
Moderate climate (**DV**)	-	1941	30692
Cold climate without ice cover (permafrost) (**CB**)	11	1540	116980
Cold climate with ice cover (glaciation) (**CG**)	63	6089	73664
Warm climate, climate change prediction W_H of KNMI (**CM2**)	6.5	1990	29785
Warm climate, Mediterranean climate (**CM**)	7.3	1802	52780

5.3.2. Dispersion

In [Valstar, 2017], it is suggested to distinguish between three dilution cases. There is a relation between dilution by dispersion and the initial flow rate, therefore [Valstar, 2017] suggests to combine the initial flow rates with the three dispersion dilution cases:

Table 5-4: Recommended dispersion dilution factors and initial flow rates for three dilution cases [Valstar, 2017]

Dispersion case	F_{disp} [-]	initial flow rate [m³/yr]	flow rate out of Overburden Q_{Ov} [m³/yr]
Little dispersion (**DV**)	4.5	4500	20’250
Intermediate dispersion (**ID**)	25	1500	37’500
Large dispersion (**LaD**)	100	150	15’000

5.3.3. Sorption parameters

The reactive behaviour of the radionuclides is represented by the retardation factor R (Eq. 5-1), analogous to the approach described in the previous chapter. In the *Overburden* compartment, transport is assumed to take place by advection rather than by diffusion. In this case colloid bound nuclides are considered to migrate at the same rate as free dissolved ions, simplifying the approach. The parameter variations considered are summarized in Table 5-5. The different range of geochemical conditions used for the *Overburden* (e.g. in pH and pe, reactivity of organic material, or bicarbonate concentrations) in comparison with those used for the *Host Rock* compartment (Table 4-4), results in different ranges of estimated retardation values. Table 5-6 summarizes the retardation factors as calculated in OPERA Task 6.2 [Rosca-Bocancea, 2017; Section 4.4]. Values in italic are conservative estimations in case no value is given, based on the lowest retardation established in [Rosca-Bocancea, 2017]. As default value (**DV**) for the **N1** case, no retardation is assumed (i.e., all R-values equals 1) [Verhoef, 2016].

Table 5-5: Geochemical parameters values used for the calculation of the retardation factors in the Overburden [Rosca-Bocancea, 2017].

Parameter	Units	Lower limit	Upper limit
pH	-	4	9
pH+pe	-	4	15
Clay	wt%	2	23
Pyrite	wt%	0.1	0.6
SHA	wt%	0.1	2.2
HFO	wt%	0	3.1
DHA	kg/l	1.0E-07	1.0E-04
Porosity	-	0.3	0.4
Density	g/cm³	2.0	2.8
Na^+	mol/l	1.0 E-02	5.0 E-01
K^+	mol/l	1.0 E-02	1.0 E-01
Cl^-	mol/l	1.0 E-02	5.0 E-01
SO_4^{2-}	mol/l	1.0 E-02	2.0 E-01
total Ca	mol/kg	1.0 E-02	7.0 E-01
total C	mol/kg	1.0 E-02	7.0 E-01
Se, U, Tc, Th, Np, I	mol/kg	1.0 E-09	1.0 E-05

Table 5-6: Default value (DV, [Verhoef, 2016]) and distributions of retardation factor for the overburden ([Rosca-Bocancea, 2017], Table 4-5 and 4-6, except italic values).

Element	Retardation factor R [-]			
	Default value (DV)	Minimum	5-percentile	Maximum
Ac	1	155	985	1.20E+06
Ag	1	1	9	1.13E+06
Am	1	155	985	1.20E+06
Ba	1	1	2	11’000
Be	1	1	9	1.13E+06
Bi	1	155	985	1.20E+06
C	1	1	1	1690
Ca	1	1	2	11’000
Cf	1	155	985	1.20E+06
Cl	*1*			
Cm	1	155	985	1.20E+06
Cd	1	1	9	1.13E+06
Cs	1	1	2	11’000
Eu	1	155	985	1.20E+06
H	*1*			
I	1	1	1	2
K	1	1	1	32
Kr	*1*			
Mo	*1*			
Nb	1	2	758	1.15E+06
Ni	1	1	9	1.13E+06
Np	1	155	1170	5.08E+06
Pa	1	2	758	1.15E+06
Pb	1	1	9	1.13E+06
Pd	1	1	9	1.13E+06
Pm	*1*			
Pu	1	155	985	1.20E+06
Ra	1	1	2	11’000
Re	1	155	985	1.20E+06
Se	1	1	1	1.60E+12
Sm	1	155	985	1.20E+06
Sn	1	1	9	1.13E+06
Sr	1	1	2	11’000
Tc	1	1	9	1.13E+06
Th	1	155	1070	2.46E+06
U	1	2	758	1.15E+06
Zr	1	1	2	11’000

6. Compartment Biosphere

6.1. General process description

In the *Biosphere* compartment, dose rates are calculated on basis of the influx of water into a fixed compartment volume. The compartment is assumed to be in steady state, i.e. the water influx equals the water outflux, with instantaneous mixing of the radionuclides entering the compartment. The concentration $C_{i,k}$ of a radionuclide i into a *Biosphere* compartment k (Figure 6-1) is calculated by

$$C_{i,k} = \frac{C_{i,ov} \cdot Q_{ov}}{Q_{flow}}$$ **Eq. 6-1**

with $C_{i,ov}$ the concentration of a radionuclide i in the *Overburden*, $Q_{,ov}$ inflow from the *Overburden* compartment directed into the subcompartment k (Table 6-1), and Q_{flow} the in- or outflow of the Biosphere subcompartment [Grupa, 2017d]. The ratio Q_{flow} / Q_{ov} is thus a dilution factor F_d and allows to calculate the concentration in the compartment according to:

$$C_{i,k} = \frac{C_{i,ov}}{F_d}$$ **Eq. 6-2**

Three Biosphere subcompartment are defined in [Grupa, 2017d] - *well*, *rivers and lakes*, and *wetlands*. The dose rate is calculated according to

$$dose\ \ rate = \sum_k \sum_i C_{i,k} \cdot DCC_{i,k}$$ **Eq. 6-3**

with $C_{i,k}$ and $DCC_{i,k}$ the concentration and *DCC*-value for each radionuclide i in subcompartment k, respectively.

6.2. Discretization of the Overburden compartment

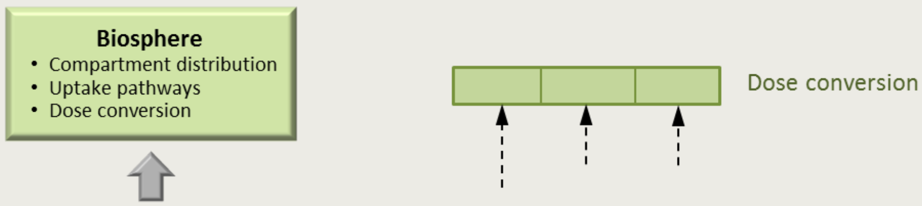

Figure 6-1: Schematic representation of the biosphere component

An overview of the links between the *Overburden* compartment and *Biosphere* subcompartments is given in Table 6-1. No indication on the distribution of the inflow over the three subcompartments is provided in any other OPERA project. Assuming that one of the three pathways is dominating, four subcases are considered in which the inflow to the biosphere follow <u>exclusively</u> one of the three routes:

- ***drinking water well case*** **(DW)**
- ***irrigation water well case*** **(DV)**
- ***rivers or lakes case*** **(RL)**
- ***wetland case*** **(WL)**

Other mixed distributions covering more than one subcompartment might be investigated as part of uncertainty analysis. The *irrigation water well case* is used to derive default values for **N1**.

The *well* subcompartment is - unlike the other subcompartments - not linked to the top cell of the *Overburden* model. Assuming that drinking or irrigation water is pumped up from a sandy, non-brackish subsurface layer, the *Peize Waalre sand 7* compartment [Valstar, 2016; Table 3.1] is selected as source layer of the well. The accompanying cell number is derived by calculating the relative travel time in the *Overburden* to the *Peize Waalre sand 7* compartment (Table 6-2), and for the sake of simplicity, for all subcases the lowest cell number of the three subcase discussed in [Valstar, 2016] is taken as interface to the *well* subcompartment.

Table 6-1: General *Biosphere* parameter

Parameter	Well	Rivers or lakes	Wetlands
related *Overburden* cell	45	50	50

Table 6-2: Flow Q_{ov} [Valstar, 2017] and model coupling for the *well* subcompartment for the fast, medium and slow streamlines for a moderate climate.

Streamline	Inflow Q_{ov} [m^3/a]	Well coupling cell [-]
Fast (**DV**)	20’250	46
Medium (**MS**)	37’500	48
Slow (**SS**)	15’000	45

6.3. Parameter values

6.3.1. Flow rates of the subcompartments

The flow rate of the *Biosphere* subcompartments, in which the influx from the *Overburden* compartment dilutes, has a large impact on the calculated risks, because it is linearly linked to the dilution assumed here (Eq. 6-1 to Eq. 6-3). The outcomes of the OPERA projects delivers insufficient basis for the derivation of realistic, conservative estimations of the subcompartments flow rates or volumes. Because these values are necessary for the safety assessments, in the next sections, values are elaborated for all subcompartments, based on a limited expert judgement. With different assumptions resulting in relevantly different estimations of the dilution factors, the numbers provided in the remainder of this section cannot be seen as robust either.

With only moderate differences between DCC-values found for the three subcompartments, and the existing uncertainty on the distribution of the influx, the subcompartment with the smallest dilution factor is expected to dominate the calculated risks. I.e. each of the subcompartments discussed in the next section needs plausible assumptions. With this in mind, several approaches are discussed, following the main guideline that the safety assessment should cover “*average member of the group of the most exposed individuals*” [Becker, 2002].

Drinking water well subcase (DW)

The *drinking water well subcase* assumes the use of a subsurface well on reasonable depth, and is comparable to the *deep well assessment case* **N5** (see Section 7.4). The release into a well is modelled as depicted in Figure 6-2 below.

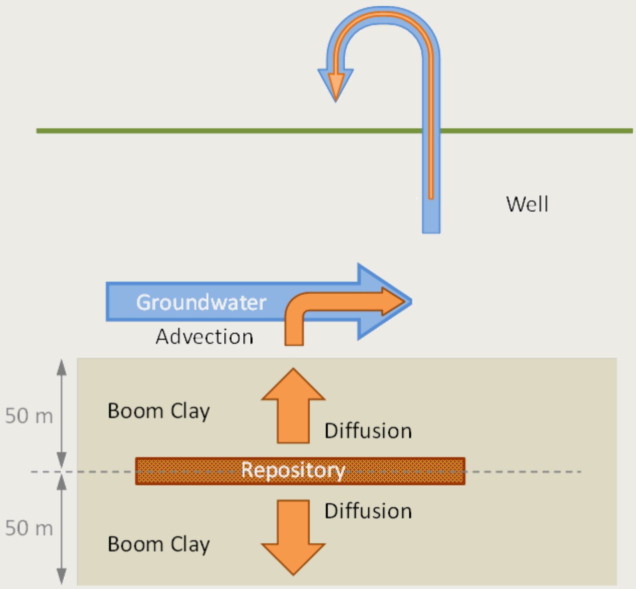

Figure 6-2: Schematic representation of water intake from a well

The aquifer above the Boom Clay is situated in unconsolidated sedimentary deposits. For typical pumping stations with 10^6 m^3/year, the well capacity is assumed to be 40-100 m^3/h equivalent to a flow Q_{flow} of $3.5{\cdot}10^5$ m^3/yr or more [Grupa, 2017d]. This value is used to define the case of a ***regional pumping station*** (**DW-R**) for domestic demands (Table 6-3).

It has been estimated that in the Netherlands about 50'000 to 150'000 local wells exists with capacities of <10 m^3/a [CIW, 1999]. Based on the abundance of such small capacity wells, a ***local well*** (**DW-L**) can be defined (Table 6-3). The well capacity is much smaller the yearly inflow from the *Overburden* to the *Biosphere* compartment, and can cover the drinking water supply of several adults (assumed annual drinking water intake of an adult: up to 1.2 m^3 [Grupa, 2017d]). Such a well at the point of maximum radionuclide concentration would lead to an undiluted intake of overburden water [Grupa, 2017d].

Table 6-3: Inflow to the *drinking water well* subcompartment and resulting dilution factor in case of a typical regional pumping station and a local well for the little dispersion, intermediate dispersion, and large dispersion case

Dispersion case	Regional pumping station (DW-R) Q_{flow} [m^3/a]	Regional pumping station (DW-R) Dilution factor F_d [-]	Local well (DW-L) Q_{flow} [m^3/a]	Local well (DW-L) Dilution factor F_d [-]
Little dispersion (**DV**)	$3.5{\cdot}10^5$	17.3	10	1
Intermediate dispersion (**ID**)	$3.5{\cdot}10^5$	9.3	10	1
Large dispersion (**LaD**)	$3.5{\cdot}10^5$	23.3	10	1

Irrigation water well subcase (IW)

Like in the previous subcase, the release into a well is modelled as indicated in Figure 6-2 above, with the well assumed to be drilled into the nuclide-bearing aquifer. The aquifer should be at an accessible depth and provide sufficient water for domestic uses. Groundwater is used as drinking water and for irrigating crops and pasture, and watering livestock [Grupa, 2017d]. The DCC-values for this subcase (Table 6-10) are based on the assumption that a self-sustaining adult needs at least 3500 m^3 water per year [Grupa, 2017d]. Comparable to the previous subcase, two variants are distinguished: a ***regional pumping station*** (**IW-R**) and a ***local well*** (**DV**), with in the latter case assuming the well to provide water for a family of four adults (i.e. an annual well capacity of 14'000 m^3).

Table 6-4: Inflow to the *well* subcompartment and resulting dilution factor in case of a typical regional pumping station and a local well for the little dispersion, intermediate dispersion, and large dispersion case

Dispersion case	Regional pumping station (IW-R)		Local well (DV)	
	Q_{flow} [m³/a]	Dilution factor F_d [-]	Q_{flow} [m³/a]	Dilution factor F_d [-]
Little dispersion (**DV**)	$3.5 \cdot 10^5$	17.3	14'000	1
Intermediate dispersion (**ID**)	$3.5 \cdot 10^5$	9.3	14'000	1
Large dispersion (**LaD**)	$3.5 \cdot 10^5$	23.3	14'000	1

Rivers or lakes subcase (RL)

The release into surface water was modelled as indicated in Figure 6-3 [Grupa, 2017d; Figure 4-2]. The surface water body represents a river, lake or pond with a given flow rate or outflow, respectively. The water is used for production of drinking water, irrigating crops and pasture, watering cattle, fishing and leisure.

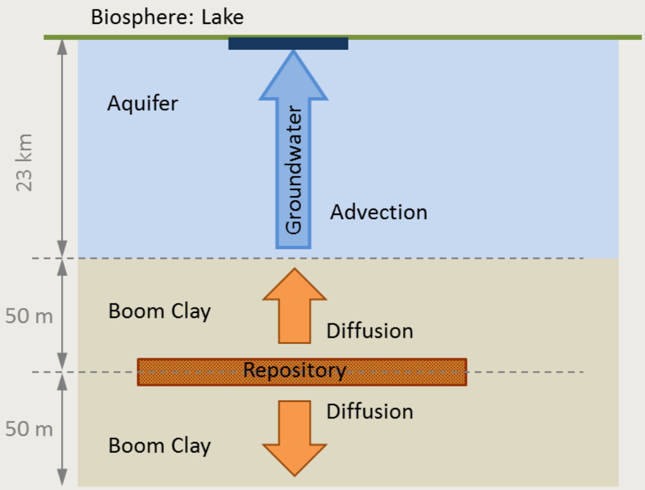

Figure 6-3: Schematic overview of a release into a river or lake

A large variety of annual river flow rates can be found in the Netherlands, with average flow rates up to $7 \cdot 10^{11}$ m^3/a [Rijkswaterstaat, 2016]. The Lek is an example for a ***large river*** (**RL-L**) with drinking water winning by river bank filtration, with a discharge of about $1 \cdot 10^{10}$ m^3/a [Rijkswaterstaat, 2016]. However, rivers can have relevantly smaller flow rates, e.g. the Linge, the longest Dutch river, has a flow rate of about $2 \cdot 10^8$ m^3/a. Although a flow rate of local streams or water channels can be relevantly smaller than that, for a ***small river*** (**RL-S**) an annual flow rate of $1 \cdot 10^6$ m^3 is assumed [Grupa, 2017d], in line with the minimum volume assumed for the DCC-values as summarized in Table 6-11.

Table 6-5: Inflow to the *rivers or lakes* subcompartment and resulting dilution factor for a larger and smaller river and for the little dispersion, intermediate dispersion, and large dispersion case

Dispersion case	Large river (RL-L)		Small river (RL-S)	
	Q_{flow} [m^3/a]	Dilution factor F_d [-]	Q_{flow} [m^3/a]	Dilution factor F_d [-]
Little dispersion (**DV**)	$1{\cdot}10^{10}$	$4.9{\cdot}10^5$	$1{\cdot}10^6$	49
Intermediate dispersion (**ID**)	$1{\cdot}10^{10}$	$2.7{\cdot}10^5$	$1{\cdot}10^6$	27
Large dispersion (**LaD**)	$1{\cdot}10^{10}$	$6.7{\cdot}10^5$	$1{\cdot}10^6$	67

Wetland subcase (WL)

The *wetland* subcase represents a system with crops and pastures. For this receptor it is assumed that the soil water in the topsoil is directly contaminated by the upwelling groundwater when the water table is high. Plants may grow on the soil and be used for food or animal feed. The release into wetland is modelled as indicated in Figure 6-4.

The *wetland* subcase represent a drained marshland (“polder”). The polder is situated in general below the surrounding water level for some of all parts of the year. Water enters the polder through rainfall or ground water, with the water level artifically maintain by pumping or draining at low tide.

The annual flow rate in this system is based on the assumption that 1/3 of the evapotranspirated water will originate from deep groundwater, and the remainder 2/3 are run off, e.g. by pumping. From Table 5-2, an interface area of the last Overburden cell with the wetland compartment can be derived of about 200 - 500 m^2 in case of vertical flow (WL-V;Table 6-6) and about 300’000 to 600’000 m^2 in case of horizontal flow (WL-H; Table 6-6). An evapotranspiration rate of 400 mm/yr lead to water flow of about 90 - 220 m^3/a and 125’000 to 250’000 m^3/a, respectively (Table 6-6). The resulting dilution factors are summarized in Table 6-7.

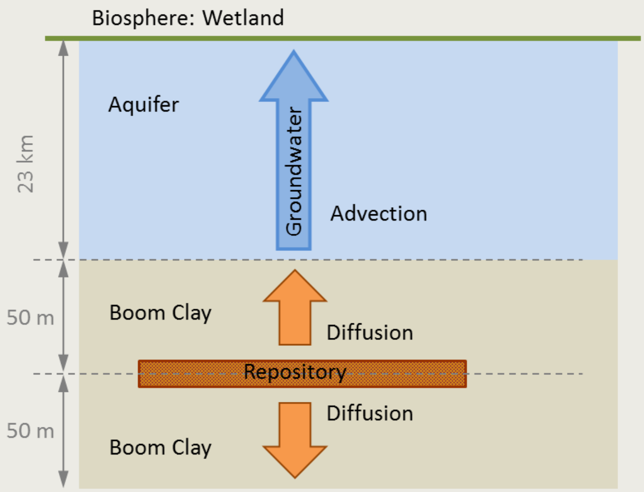

Figure 6-4: Schematic overview of wetland receptor

Table 6-6: Horizontal and vertical area of the interface *Overburden* - wetland for the fast, medium and slow streamlines and the little dispersion, intermediate dispersion, and large dispersion case

Area [m^2] Vertical flow case / Horizontal flow case	Fast streamline (DV)	Medium streamline (MS)	Slow streamline (SS)
Little dispersion (**DV**)	70'200 / 512’600	624'200 / 308’000	1'611'900 / 620’400
Intermediate dispersion (**ID**)	130'000 / 512’600	115'600 / 308’000	2'985'000 / 620’400
Large dispersion (**LaD**)	52'000 / 512’600	462'400/ 308’000	1'194'000 / 620’400

Table 6-7: Inflow to the *wetlands* subcompartment and resulting dilution factor for vertical and horizontal coupling of the Overburden and the little dispersion, intermediate dispersion, and large dispersion case

Dispersion case	Vertical flow (WL-V)*		Horizontal flow (WL-H)*	
	Q_{flow} [m^3/a]	Dilution factor F_d [-]	Q_{flow} [m^3/a]	Dilution factor F_d [-]
Little dispersion (**DV**)	28'100/52'000 /20'800	4.2/37/96	205’000/123’000 /248’000	30.4/18.2/36.7
Intermediate dispersion (**ID**)	250'000/462'000 /185'000			16.4/9.8/19.8
Large dispersion (**LaD**)	645'000/1'195'000 /478'000			41.0/24.6/49.6

* for fast/medium/slow streamline

Table 6-8 summarizes the dilution factors calculated for all subcases.

Table 6-8: Overview of dilution factors for all subcases and for the fast, medium and slow streamlines

Dispersion case	Dilution factor F_d [-]							
	Drinking water well subcase (DW)		Irrigation water well subcase (IW)		Rivers or lakes subcase (RL)		Wetlands subcase (WL)*	
	Regional pumping station (DW-R)	Local well (DW-L)	Regional pumping station (DV)	Local well (IW-L)	Large river (RL-L)	Small river (RL-S)	Vertical flow (WL-V)	Horizontal flow (WL-H)
Little dispersion (**DV**)	17.3	1	17.3	1	$4.9 \cdot 10^5$	49	4.2/37 /96	30.4/18.2/36.7
Intermediate dispersion (**ID**)	9.3	1	9.3	1	$2.7 \cdot 10^5$	27		16.4/9.8/19.8
Large dispersion (**LaD**)	23.3	1	23.3	1	$6.7 \cdot 10^5$	67		41.0/24.6/49.6

* for fast/medium/slow streamline

6.3.2. Dose conversion factors

For the OPERA analyses, *dose conversion coefficients* (DCC) are determined in [Grupa, 2017d]. Table 6-9 to Table 6-12 summarizes the DCC-values for the considered subcases. Missing values for a number of radionuclides in Table 6-9 to Table 6-12 are completed in a conservative manner: the highest ratio of the DCC-values and $e_{50(ing)}$ [ICRP, 2012] found in a column is multiplied with the $e_{50(ing)}$ of the radionuclide j of interest:

$$DCC_{j,k} = \max\left|\frac{DCC_i}{e_{50(ing),i}}\right| e_{50(ing),j} \qquad \textbf{Eq. 6-4}$$

These added values are marked in italic. The DCC-values in Table 6-9 are based on the $e_{50(ing)}$ for adults [ICRP, 2012], assuming a drinking water intake of 0.74 m^3/yr [Grupa, 2017d] for the temperate (**DV**) and boreal climate (**BC**), and 1.2 m^3/yr for the Mediterranean climate (**MC**).

Compared to the general uncertainties of these values, the uncertainty between the three climates is rather small: the DCC-values provided for a particular radionuclide varies by a factor of 6 to 8 (data not shown). The Mediterranean climate results in the highest values for the majority of the DCC-values, and the boreal climate result in lower values than the moderate or Mediterranean climate in all cases, making this climate evolution the least critical.

Table 6-9: Dose conversion coefficients for an adult for the *drinking water well subcase* (DW) and three climate subcases (based on [ICRP, 2012], except italic values)

Radionuclide	*DCC* [Sv/y per Bq/m³]		
	Temperate climate (TC)	Mediterranean climate (MC)	Boreal climate (BC)
^{227}Ac	8.10E-07	1.32E-06	8.10E-07
^{108m}Ag	1.69E-09	2.76E-09	1.69E-09
^{241}Am	1.47E-07	2.40E-07	1.47E-07
^{242m}Am	1.40E-07	2.28E-07	1.40E-07
^{243}Am	1.47E-07	2.40E-07	1.47E-07
^{133}Ba	1.10E-09	1.80E-09	1.10E-09
^{10}Be	8.10E-10	1.32E-09	8.10E-10
^{207}Bi	9.57E-10	1.56E-09	9.57E-10
^{14}C	4.27E-10	6.96E-10	4.27E-10
^{41}Ca	1.40E-10	2.28E-10	1.40E-10
^{249}Cf	2.58E-07	4.20E-07	2.58E-07
^{36}Cl	6.84E-10	1.12E-09	6.84E-10
^{243}Cm	1.10E-07	1.80E-07	1.10E-07
^{244}Cm	8.83E-08	1.44E-07	8.83E-08
^{245}Cm	1.55E-07	2.52E-07	1.55E-07
^{246}Cm	1.55E-07	2.52E-07	1.55E-07
^{247}Cm	1.40E-07	2.28E-07	1.40E-07
^{248}Cm	5.67E-07	9.24E-07	5.67E-07
^{113m}Cd	1.69E-08	2.76E-08	1.69E-08
^{135}Cs	1.47E-09	2.40E-09	1.47E-09
^{137}Cs	9.57E-09	1.56E-08	9.57E-09
^{152}Eu	1.03E-09	1.68E-09	1.03E-09
^{3}H	1.32E-11	2.16E-11	1.32E-11
^{129}I	8.10E-08	1.32E-07	8.10E-08
^{40}K	4.56E-09	7.44E-09	4.56E-09
^{81}Kr	*n.d.*	*n.d.*	*n.d.*
^{85}Kr	*n.d.*	*n.d.*	*n.d.*
^{93}Mo	2.28E-09	3.72E-09	2.28E-09
^{93m}Nb	8.83E-11	1.44E-10	8.83E-11
^{94}Nb	1.25E-09	2.04E-09	1.25E-09
^{59}Ni	4.64E-11	7.56E-11	4.64E-11
^{63}Ni	1.10E-10	1.80E-10	1.10E-10
^{237}Np	8.10E-08	1.32E-07	8.10E-08
^{231}Pa	5.23E-07	8.52E-07	5.23E-07
^{210}Pb	5.08E-07	8.28E-07	5.08E-07
^{107}Pd	2.72E-11	4.44E-11	2.72E-11
^{145}Pm	8.10E-11	1.32E-10	8.10E-11
^{238}Pu	1.69E-07	2.76E-07	1.69E-07
^{239}Pu	1.84E-07	3.00E-07	1.84E-07
^{240}Pu	1.84E-07	3.00E-07	1.84E-07
^{241}Pu	3.53E-09	5.76E-09	3.53E-09
^{242}Pu	1.77E-07	2.88E-07	1.77E-07
^{244}Pu	1.77E-07	2.88E-07	1.77E-07
^{226}Ra	2.06E-07	3.36E-07	2.06E-07
^{186m}Re	1.62E-09	2.64E-09	1.62E-09
^{79}Se	2.13E-09	3.48E-09	2.13E-09
^{151}Sm	7.21E-11	1.18E-10	7.21E-11
^{121m}Sn	2.80E-10	4.56E-10	2.80E-10
^{126}Sn	3.46E-09	5.64E-09	3.46E-09
^{90}Sr	2.06E-08	3.36E-08	2.06E-08
^{99}Tc	4.71E-10	7.68E-10	4.71E-10
^{229}Th	3.61E-07	5.88E-07	3.61E-07
^{230}Th	1.55E-07	2.52E-07	1.55E-07
^{232}Th	1.69E-07	2.76E-07	1.69E-07
^{232}U	2.43E-07	3.96E-07	2.43E-07
^{233}U	3.75E-08	6.12E-08	3.75E-08
^{234}U	3.61E-08	5.88E-08	3.61E-08
^{235}U	3.46E-08	5.64E-08	3.46E-08
^{236}U	3.46E-08	5.64E-08	3.46E-08
^{238}U	3.31E-08	5.40E-08	3.31E-08
^{93}Zr	8.10E-10	1.32E-09	8.10E-10

Table 6-10: Dose conversion coefficients for an adult calculated for the *irrigation water well subcase* (IW) and three climate subcases ([Grupa, 2017d], except italic values)

Radionuclide	*DCC* [Sv/y per Bq/m^3]		
	Temperate climate (DV)	Mediterranean climate (MC)	Boreal climate (BC)
^{227}Ac	1.55E-06	3.50E-06	1.10E-06
^{108m}Ag	1.26E-08	1.38E-08	4.36E-09
^{241}Am	2.28E-07	5.44E-07	1.60E-07
^{242m}Am	2.27E-07	5.27E-07	1.59E-07
^{243}Am	2.47E-07	6.83E-07	1.71E-07
^{133}Ba	*1.88E-08*	*2.31E-08*	*5.95E-09*
^{10}Be	1.40E-09	3.37E-09	9.59E-10
^{207}Bi	*1.63E-08*	*2.00E-08*	*5.16E-09*
^{14}C	4.65E-10	5.24E-10	4.29E-10
^{41}Ca	2.74E-10	6.06E-10	1.95E-10
^{249}Cf	*4.39E-06*	*5.38E-06*	*1.39E-06*
^{36}Cl	2.73E-09	8.55E-09	1.35E-09
^{243}Cm	*1.88E-06*	*2.31E-06*	*5.95E-07*
^{244}Cm	1.36E-07	3.11E-07	9.53E-08
^{245}Cm	2.52E-07	7.04E-07	1.77E-07
^{246}Cm	2.47E-07	6.74E-07	1.75E-07
^{247}Cm	*2.38E-06*	*2.92E-06*	*7.54E-07*
^{248}Cm	9.27E-07	2.76E-06	6.57E-07
^{113m}Cd	*2.88E-07*	*3.54E-07*	*9.13E-08*
^{135}Cs	5.26E-09	1.21E-08	3.64E-09
^{137}Cs	2.68E-08	5.68E-08	1.93E-08
^{152}Eu	*1.75E-08*	*2.15E-08*	*5.56E-09*
^{3}H	*2.26E-10*	*2.77E-10*	*7.15E-11*
^{129}I	1.32E-07	3.39E-07	1.08E-07
^{40}K	1.28E-08	2.77E-08	9.26E-09
^{81}Kr	*n.d.*	*n.d.*	*n.d.*
^{85}Kr	*n.d.*	*n.d.*	*n.d.*
^{93}Mo	4.64E-09	1.12E-08	3.08E-09
^{93m}Nb	*1.50E-09*	*1.85E-09*	*4.76E-10*
^{94}Nb	2.13E-08	1.44E-08	4.12E-09
^{59}Ni	9.08E-11	2.17E-10	5.87E-11
^{63}Ni	2.01E-10	4.61E-10	1.38E-10
^{237}Np	1.26E-07	2.88E-07	8.82E-08
^{231}Pa	1.48E-06	6.10E-06	9.09E-07
^{210}Pb	8.89E-07	2.00E-06	6.52E-07
^{107}Pd	6.28E-11	1.59E-10	3.85E-11
^{145}Pm	*1.38E-09*	*1.69E-09*	*4.37E-10*
^{238}Pu	2.61E-07	6.01E-07	1.83E-07
^{239}Pu	2.90E-07	7.44E-07	2.04E-07
^{240}Pu	2.89E-07	7.33E-07	2.04E-07
^{241}Pu	5.44E-09	1.24E-08	3.81E-09
^{242}Pu	2.79E-07	7.18E-07	1.96E-07
^{244}Pu	3.21E-07	7.39E-07	2.03E-07
^{226}Ra	5.96E-07	1.33E-06	3.61E-07
^{186m}Re	*2.76E-08*	*3.38E-08*	*8.73E-09*
^{79}Se	1.61E-08	4.46E-08	8.82E-09
^{151}Sm	*1.23E-09*	*1.51E-09*	*3.89E-10*
^{121m}Sn	*4.76E-09*	*5.84E-09*	*1.51E-09*
^{126}Sn	2.80E-08	2.82E-08	7.98E-09
^{90}Sr	3.90E-08	1.76E-07	4.30E-08
^{99}Tc	7.66E-10	1.78E-09	5.38E-10
^{229}Th	7.52E-07	1.97E-06	5.22E-07
^{230}Th	2.58E-07	7.03E-07	1.81E-07
^{232}Th	1.41E-06	3.27E-06	9.13E-07
^{232}U	5.45E-07	1.24E-06	3.81E-07
^{233}U	5.92E-08	1.37E-07	4.15E-08
^{234}U	5.69E-08	1.31E-07	3.99E-08
^{235}U	5.55E-08	1.27E-07	3.86E-08
^{236}U	5.46E-08	1.26E-07	3.82E-08
^{238}U	5.63E-08	1.30E-07	3.94E-08
^{93}Zr	1.86E-09	4.08E-09	1.33E-09

Table 6-11: Dose conversion coefficients for an adult calculated for the *rivers or lakes* sub*case* (RL) and three climate subcases ([Grupa, 2017d], except italic values)

Radionuclide	*DCC* [Sv/y per Bq/m^3]		
	Temperate climate (DV)	Mediterranean climate (MC)	Boreal climate (BC)
^{227}Ac	9.51E-07	2.90E-06	4.99E-07
^{108m}Ag	2.46E-07	1.84E-07	2.37E-07
^{241}Am	1.30E-07	4.45E-07	6.19E-08
^{242m}Am	1.30E-07	4.29E-07	6.16E-08
^{243}Am	1.75E-07	6.03E-07	9.89E-08
^{133}Ba	*1.60E-07*	*1.20E-07*	*1.55E-07*
^{10}Be	1.74E-09	3.70E-09	1.29E-09
^{207}Bi	*1.39E-07*	*1.04E-07*	*1.34E-07*
^{14}C	1.84E-08	1.85E-08	1.84E-08
^{41}Ca	3.19E-10	6.51E-10	2.39E-10
^{249}Cf	*3.74E-05*	*2.80E-05*	*3.61E-05*
^{36}Cl	3.02E-09	8.84E-09	1.63E-09
^{243}Cm	*1.60E-05*	*1.20E-05*	*1.55E-05*
^{244}Cm	1.14E-07	2.90E-07	7.36E-08
^{245}Cm	2.16E-07	6.67E-07	1.40E-07
^{246}Cm	2.09E-07	6.36E-07	1.37E-07
^{247}Cm	*2.03E-05*	*1.52E-05*	*1.96E-05*
^{248}Cm	7.88E-07	2.62E-06	5.18E-07
^{113m}Cd	*2.46E-06*	*1.84E-06*	*2.37E-06*
^{135}Cs	1.72E-08	2.41E-08	1.56E-08
^{137}Cs	1.45E-07	1.64E-07	1.37E-07
^{152}Eu	*1.50E-07*	*1.12E-07*	*1.44E-07*
^{3}H	*1.93E-09*	*1.44E-09*	*1.85E-09*
^{129}I	2.00E-07	4.07E-07	1.76E-07
^{40}K	6.44E-08	7.54E-08	6.08E-08
^{81}Kr	*n.d.*	*n.d.*	*n.d.*
^{85}Kr	*n.d.*	*n.d.*	*n.d.*
^{93}Mo	4.52E-09	1.11E-08	2.96E-09
^{93m}Nb	*1.28E-08*	*9.60E-09*	*1.24E-08*
^{94}Nb	2.84E-08	2.02E-08	1.13E-08
^{59}Ni	1.17E-10	2.43E-10	8.45E-11
^{63}Ni	2.63E-10	5.23E-10	2.00E-10
^{237}Np	1.32E-07	2.94E-07	9.46E-08
^{231}Pa	1.28E-06	5.90E-06	7.08E-07
^{210}Pb	7.07E-07	1.81E-06	6.74E-07
^{107}Pd	5.15E-11	1.48E-10	2.72E-11
^{145}Pm	*1.18E-08*	*8.80E-09*	*1.13E-08*
^{238}Pu	1.52E-07	4.93E-07	7.44E-08
^{239}Pu	1.72E-07	6.26E-07	8.63E-08
^{240}Pu	1.71E-07	6.15E-07	8.56E-08
^{241}Pu	3.17E-09	1.02E-08	1.55E-09
^{242}Pu	1.65E-07	6.05E-07	8.31E-08
^{244}Pu	4.11E-07	7.74E-07	2.93E-07
^{226}Ra	7.05E-07	1.43E-06	4.70E-07
^{186m}Re	*2.35E-07*	*1.76E-07*	*2.27E-07*
^{79}Se	1.97E-08	4.82E-08	1.24E-08
^{151}Sm	*1.05E-08*	*7.84E-09*	*1.01E-08*
^{121m}Sn	*4.06E-08*	*3.04E-08*	*3.92E-08*
^{126}Sn	2.78E-07	2.23E-07	2.58E-07
^{90}Sr	4.00E-08	1.64E-07	3.10E-08
^{99}Tc	8.25E-10	1.84E-09	5.98E-10
^{229}Th	8.67E-07	2.08E-06	6.38E-07
^{230}Th	2.85E-07	7.29E-07	2.08E-07
^{232}Th	1.93E-06	3.69E-06	1.43E-06
^{232}U	5.57E-07	1.25E-06	3.93E-07
^{233}U	5.84E-08	1.36E-07	4.07E-08
^{234}U	5.61E-08	1.30E-07	3.91E-08
^{235}U	5.63E-08	1.27E-07	3.93E-08
^{236}U	5.38E-08	1.25E-07	3.75E-08
^{238}U	5.58E-08	1.29E-07	3.89E-08
^{93}Zr	2.92E-09	5.14E-09	2.40E-09

Table 6-12: Dose conversion coefficients for an adult calculated for the *wetland subcase* (WL) and three climate subcases ([Grupa, 2017d], except italic values)

Radionuclide	*DCC* [Sv/y per Bq/m³]		
	Temperate climate (DV)	Mediterranean climate (MC)	Boreal climate (BC)
^{227}Ac	1.05E-06	2.04E-06	1.24E-06
^{108m}Ag	3.91E-08	8.66E-09	1.27E-08
^{241}Am	4.17E-08	2.46E-07	8.49E-08
^{242m}Am	4.23E-08	2.42E-07	8.40E-08
^{243}Am	7.21E-08	2.46E-07	9.28E-08
^{133}Ba	*4.36E-08*	*2.95E-08*	*2.64E-08*
^{10}Be	5.01E-10	6.47E-10	4.96E-10
^{207}Bi	*3.78E-08*	*2.56E-08*	*2.29E-08*
^{14}C	9.13E-11	9.13E-11	9.13E-11
^{41}Ca	2.45E-11	2.48E-11	2.39E-11
^{249}Cf	*1.02E-05*	*6.89E-06*	*6.16E-06*
^{36}Cl	1.50E-08	1.42E-08	1.43E-08
^{243}Cm	*4.36E-06*	*2.95E-06*	*2.64E-06*
^{244}Cm	2.40E-08	1.41E-07	4.95E-08
^{245}Cm	4.99E-08	2.24E-07	8.21E-08
^{246}Cm	3.90E-08	2.22E-07	7.87E-08
^{247}Cm	*5.52E-06*	*3.74E-06*	*3.34E-06*
^{248}Cm	1.41E-07	7.94E-07	2.83E-07
^{113m}Cd	*6.68E-07*	*4.53E-07*	*4.04E-07*
^{135}Cs	6.23E-09	6.76E-09	5.94E-09
^{137}Cs	6.94E-08	4.97E-08	4.75E-08
^{152}Eu	*4.07E-08*	*2.76E-08*	*2.46E-08*
^{3}H	*5.23E-10*	*3.54E-10*	*3.17E-10*
^{129}I	2.45E-09	2.48E-09	2.28E-09
^{40}K	2.27E-09	2.17E-09	2.16E-09
^{81}Kr	*n.d.*	*n.d.*	*n.d.*
^{85}Kr	*n.d.*	*n.d.*	*n.d.*
^{93}Mo	3.65E-09	3.64E-09	3.62E-09
^{93m}Nb	*3.49E-09*	*2.36E-09*	*2.11E-09*
^{94}Nb	4.94E-08	1.01E-08	1.54E-08
^{59}Ni	7.48E-11	8.00E-11	7.10E-11
^{63}Ni	1.78E-10	1.90E-10	1.69E-10
^{237}Np	8.01E-10	1.15E-09	7.84E-10
^{231}Pa	3.58E-06	5.94E-06	4.06E-06
^{210}Pb	1.71E-07	1.58E-07	1.57E-07
^{107}Pd	9.29E-11	9.43E-11	9.23E-11
^{145}Pm	*3.20E-09*	*2.17E-09*	*1.93E-09*
^{238}Pu	1.61E-08	9.58E-08	3.35E-08
^{239}Pu	1.75E-08	1.04E-07	3.64E-08
^{240}Pu	1.75E-08	1.04E-07	3.64E-08
^{241}Pu	3.23E-10	1.88E-09	6.63E-10
^{242}Pu	1.68E-08	1.00E-07	3.49E-08
^{244}Pu	1.20E-07	1.19E-07	6.60E-08
^{226}Ra	6.83E-06	4.97E-06	4.81E-06
^{186m}Re	*6.39E-08*	*4.33E-08*	*3.87E-08*
^{79}Se	5.53E-08	5.71E-08	5.10E-08
^{151}Sm	*2.85E-09*	*1.93E-09*	*1.72E-09*
^{121m}Sn	*1.10E-08*	*7.48E-09*	*6.68E-09*
^{126}Sn	5.62E-08	1.54E-08	2.05E-08
^{90}Sr	9.27E-09	5.63E-08	2.25E-08
^{99}Tc	1.09E-10	1.08E-10	1.08E-10
^{229}Th	2.42E-07	5.32E-07	2.85E-07
^{230}Th	7.24E-08	1.81E-07	9.46E-08
^{232}Th	6.42E-07	6.12E-07	4.63E-07
^{232}U	5.62E-08	5.27E-08	4.17E-08
^{233}U	3.77E-09	4.69E-09	3.64E-09
^{234}U	3.62E-09	4.52E-09	3.50E-09
^{235}U	4.97E-09	4.57E-09	3.81E-09
^{236}U	3.47E-09	4.28E-09	3.35E-09
^{238}U	3.85E-09	4.36E-09	3.50E-09
^{93}Zr	9.69E-12	1.12E-11	9.94E-12

7. Normal evolution assessment cases N2 - N5

In this chapter, parameter values for the *Normal evolution assessment cases* **N2** - **N5** are described in case these deviates from the values of the **N1** case as discussed in the previous sections.

7.1. Radioactive gas transport case (N2)

The general outline of this case is described in [Grupa, 2017c]. The consideration for adopting this assessment case is that gas, generated in the repository by processes like corrosion, organic degradation, or volatilisation, may potentially drive advective flow and the flow of radioactive gases which are released from the waste packages. Insufficient data is available to evaluate this process quantitatively as part of the *Normal evolution scenario,* and it is therefore not addressed further in this report. A qualitative argumentation on the relevance of this process in support of the OPERA PA is provided in [Grupa, 2017c].

7.2. Gas pressure build-up case (N3)

The general outline of this case is described in [Grupa, 2017c]. In case processes like corrosion, organic degradation, or volatilisation generates gas that is not able to disperse sufficiently through the engineered barriers or the host rock, a build-up of gas pressure may be induced. Although in principle the facility must be designed to handle a moderate build-up of gas pressure, potentially this process may impact several of the safety functions. Assuming that the gas pressure build-up is limited, this process is considered part case of the *Normal evolution scenario* [Grupa, 2017c]. Excessive gas pressure build-up is considered elsewhere as a separate What-If case.

Insufficient data is available to evaluate this process quantitatively as part of the *Normal evolution scenario,* and it is therefore not addressed further in this report. A qualitative argumentation on the relevance of this process in support of the OPERA PA is provided in [Grupa, 2017c].

7.3. Early canister failure case (N4)

A gradual degradation of steel and concrete in the EBS is part of the *Normal evolution scenario*. However, increased corrosion rates can cause early failures of the waste canister, e.g. as a result of stress-corrosion cracking as pointed out in Section 3.3.3. Also quality problems during the construction of the waste package may lead to early canister failure. Early canister failure may potentially impact the safety functions *loss of integrity of container* (*C1*), and indirectly the safety function *limitation of contaminated release from waste forms* (*R1*). The results of the **N4** case are can be compared with the **N1** central case in order to determine the potential impact of early canister failure.

In the assessment of case **N4** it is assumed that 10% of the canisters in the *Vitrified HLW* section, the *Spent Fuel* section, the *Non-heat-generating HLW* section, and the *Depleted uranium* section fails at $t_{failure}$ = 0 (Table 7-1). The other 90% of the containers fail at the timesteps as defined in **N1**:

Table 7-1: Times of container failure and release rates for the *Central assessment case* N1 and the *Early canister failure case* N4

Disposal Section	Time of container failure $t_{failure}$ [a]			Release rate λ_{rel} [1/a]
	N1	N4		
		10%	100%	N1 and N4
Vitrified HLW	35'000	0	35'000	$5.2{\cdot}10^{-5}$
Spent Fuel	35'000	0	35'000	∞
Non-heat-generating HLW	35'000	0	35'000	∞
DepU	1500	0	1500	∞
LILW	0	0	0	∞

All other parameters are set to the default value of **N1**. Excessive early canister failure (i.e. the early failure of more than one container) has been identified as a *What-If case* and will be addressed as altered scenario.

7.4. Deep well assessment case (N5)

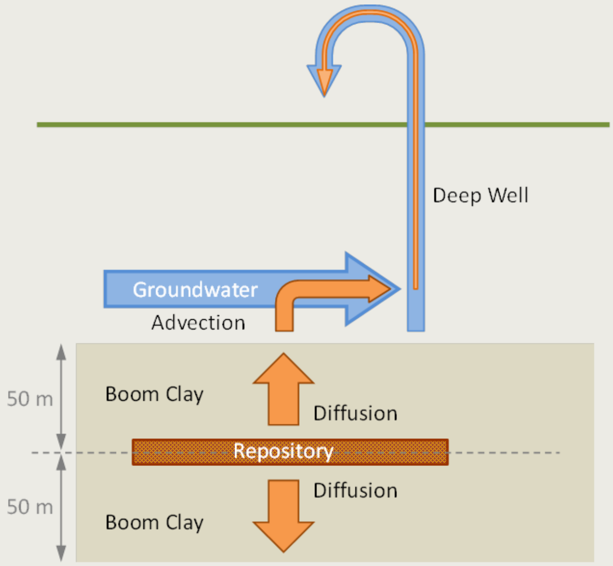

Figure 7-1: Schematic representation of water intake from a deep well

The general outline of this case is described in [Grupa, 2017c]. This case is very comparable to the *drinking water well case* (**DW**) of **N1** (see Section 6.3.1), except that the well is assumed to be situated in a considerable depth (100 to 300 m according to Grupa, 2017c), with the delayed transport through the overburden (partially) short-cutted. In case of a regional pumping station, pore volumes comparable to the *drinking water well subcase* (**DW**) of **N1** (Table 6-3) can be used. The case of the presence of a small, local well at such considerable depth is judged to be less realistic. The main difference here is that the model representation links the *Biosphere* compartment to a lower cell of the *Overburden* compartment.

The interface between brackish and fresh groundwater varies in the Netherlands between 0 to >800 m. Comparable variations are also seen in the depth of the different formations (see e.g. [Valstar, 2016]). For the generic, site-independent safety assessments it is therefore difficult to pinpoint a specific depth of a deep well in a freshwater aquifer. It is also likely that residence times are not independent from the interface fresh - brackish groundwater.

For the depth of the well of the **N5** case therefore 3/5 of the *Overburden* model is assumed (Table 7-2), independent of the properties of the related groundwater layer (and in contrast to the *drinking water well case* (**DW**) of **N1**, which is situated in the Peize sand, see Section 5.3.1).

Wells deeper than 200 m are unlikely and therefore treated as *Altered evolution*.

Table 7-2: Coupling *Overburden - well* subcompartment for the N5 case

Parameter	N1	N5
related *Overburden* cell	45	30

8. Concluding remarks

The present report lists the input parameters that are required for the ORCHESTRA computer code to perform the OPERA safety assessment.

For the *central assessment case* (**N1**) the required input parameters, their ranges and recommended default values are reported. Several subcases that are distinguished are summarized in the table below:

Table 8-1: Subcases identified as part of the *central assessment case* N1 of the *Normal evolution scenario*

Compartment	Subcases	
Waste-EBS	• *Failure base case (**DV**)* • *Early container failure case (**EF**)* • *Late container failure case (**LF**)*	
	• *Release base case (**DV**)* • *Slow release case (**SR**)* • *Fast release case (**FR**)*	
	• *Solubility base case (**DV**)* • *Low solubility case (**LS**)*	
Host rock	• *DOC base case (**DV**)* • *High DOC case (**HD**)* • *Low DOC case (**LD**)*	
Overburden	• *Fast streamline (**DV**)* • *Medium streamline (**MS**)* • *Slow streamline (**SS**)*	
	• *Little dispersion case (**DV**)* • *Intermediate dispersion case (**ID**)* • *Large dispersion case (**LaD**)*	
	• *Present day climate (**DV**) ** • *Cold climate without ice cover (permafrost) (**BC**) *** • *Cold climate with ice cover (glaciation) (**GC**)* • *Warm climate, climate change prediction WH of KNMI (**CM2**)* • *Warm climate, Mediterranean climate (**CM**) ****	
Biosphere	• *Temperate climate case (**DV**)* • *Mediterranean climate case (**CM**)* • *Boreal climate case (**BC**)*	
	• *Drinking water well case (**DW**)*	• *Regional pumping station case (**DW-R**)* • *Local well case (**DW-L**)*
	• *Irrigation water well case(**IW**)*	• *Regional pumping station case (**IW-R**)* • *Local well case (**DV**)*
	• *Rivers or lakes case (**RL**)*	• *Large river case (**RL-L**)* • *Small river case (**RL-S**)*
	• *Wetland case (**WL**)*	• *Vertical flow case (**WL-V**)* • *Horizontal flow case (**WL-H**)*

* comparable to the *Temperate climate case* in the *Biosphere*
** comparable to the *Boreal climate case* in the *Biosphere*
*** comparable to the *Mediterranean climate case* in the *Biosphere*

From the other cases of the *Normal evolution scenario*, no information is currently available to provide parameter values for the *Radioactive gas transport case* (**N2**) and the

Gas pressure build-up case (**N3**). For the *Early canister failure case* (**N4**) and the *Deep well assessment case* (**N5**), parameter values are provided.

9. References

[Arnold, 2015] Arnold, P, PJ Vardon, MA Hicks, J Fokkens, PA Fokker, *A numerical and reliability-based investigation into the technical feasibility of a Dutch radioactive waste repository in Boom Clay*, OPERA report OPERA-PU-TUD311, January 2015, 1-316.

[Becker, 2002] Becker D-A, Buhmann D, Storck R,. Alonso J, Cormenzana J-L, Hugi M, van Gemert F, O'Sullivan P, Laciok A, Marivoet J, Sillen X, Nordman H, Vieno T, Niemeyer M , Testing of Safety and Performance Indicators (SPIN), EC, EUR 19965 EN, 2002, 1-94.

[Becker, 2014] Becker D-A, Grupa JB, Wolf, J, *Methods for uncertainty analysis*, OPERA report OPERA-PU-GRS7321, December 2014.

[Berner, 2014] Berner, U, Solubility of Radionuclides in a Concrete Environment for Provisional Safety Analyses for SGT-E2, Nagra Technical Report 14-07, August 2014, 1-81.

[Beek, 2009] van Beek CGEM, de Zwart AH, Balemans M, Kooiman JW, van Rosmalen C, Timmer H, Vandersluys J, Stuyfzand PJ, *Concentration and size distribution of particles in abstracted groundwater*, Water Research, 868-878, 2009.

[Beerten, 2011] Beerten K, 2011, *Permafrost in northwestern Europe during the Last Glacial*, , SCK•CEN report ER-138, Mol , Belgium, March 2011.

[Bense, 2003] Bense V, van Balen R, de Vries J, *The impact of faults on the hydrogeological conditions in the Roer Valley Rift System: an overview*, Netherlands Journal of Geosciences / Geologie en Mijnbouw 82 (1): 41-54, 2003.

[CLO, 2016] Compendium voor de Leefomgeving, *Jaarlijkse hoeveelheid neerslag in Nederland, 1910-2015, http://www.clo.nl/indicatoren/nl0508-jaarlijkse-hoeveelheid-neerslag-in-nederland*, last accessed: 26 July 2016.

[CIW, 1999] Commissie Integraal Waterbeheer (ciw), *Kleine Grondwaterwinningen. Advies over de aanpak van de toename van kleine grondwaterwinningen*, werkgroep IV, CUWVO, May 1999.

[ICRP, 2012] International Commission on Radiological Protection (ICRP), *Compendium of Dose Coefficients based on ICRP Publication 60*, ICRP Publication 119, 2012.

[Deissmann, 2016a] Deissmann, G, K Haneke, A Filby, R Wiegers, *HLW glass dissolution*, OPERA report OPERA-PU-IBR511A, 2016, 1-71.

[Deissmann, 2016b] Deissmann, G, K Haneke, A Filby, R Wiegers, *Corrosion of spent research reactor fuels*, OPERA report OPERA-PU-IBR511B, 2016, 1-64.

[Filby, 2016] Filby, A, G Deissmann, R Wiegers, *LILW degradation processes and products*, OPERA report OPERA-PU-IBR512, October 2016, 1-145.

[Govaerts, 2015] Govaerts J, Beerten K, Ten Veen J, 2015. *Numerical simulation of Permafrost Depth in the Netherlands*, SCK•CEN-R-5848, 44 pages.

[Griffioen, 2015] Griffioen, J, *The composition of deep groundwater in the Netherlands in relation to disposal of radioactive waste*, OPERA report OPERA-PU-TNO521-2, April 2015, 1-51.

[Grupa, 2000] Grupa JB, Houkema M, *Terughaalbare opberging van radioactief afval in diepe zout en kleiformaties; Modellen voor een veiligheidsstudie*, Petten, NRG 21082/00.33017/P, March 2000.

[Grupa, 2012] Grupa JB, *OPERA Performance Assessment Project I (OPAP-I), Revised proposal for Work Package 7: scenario development and performance assessment - 3rd revision*, OPERA- RP-NRG711&712&721&731&732&733, Petten, 8 March 2012.

[Grupa, 2014] Grupa JB, *Report on the safety assessment methodology*, OPERA report OPERA-PU-NRG2121, April 2014.

[Grupa, 2017a] Grupa J.B., Meeussen J.C.L., Rosca-Bocancea E. (NRG), Buhmann D., Laggiard E. (GRS), Wildenborg A. F. B. (TNO), *Report on migration model in Boom Clay*, OPERA report OPERA-PU-NRG7212, March 2017.

[Grupa, 2017b] Grupa JB, Meeussen JCL, Rosca-Bocancea E (NRG), Wildenborg AFB, Buhmann D, Laggiard E(GRS), *Report on migration model in rock formations surrounding the host rock*, OPERA report OPERA-PU-GRS7222, January 2017.

[Grupa, 2017c] Grupa JB, J Hart, T Wildenborg, *Final report on the description of relevant scenarios for the OPERA reference concept in Boom Clay*, OPERA report OPERA-PU-NRG7111, April 2017.

[Grupa, 2017d] Grupa JB, Hart J, Meeussen HCL, Rosca-Bocancea E, Sweeck L, Wildenborg AFB, *Migration and uptake of radionuclides in the biosphere. PA-model 'Biosphere'*, OPERA report OPERA-PU-SCK631&NRG7232, February 2017.

[Hart, 2014] Hart J, *Report on the determination of the inventory*, OPERA report OPERA-PU-NRG1112A, Juni 2015.

[Hart, 2016] Hart J, TJ Schröder, *Report on alternative waste scenarios*, OPERA report OPERA-PU-NRG1121, July 2016.

[IAEA, 2004] International Atomic Energy Agency, *Safety Assessment Methodologies for Near Surface Disposal Facilities (ISAM), Vol. I – Review and Enhancement of Safety Assessment Approaches and Tools*; ISBN 92–0–104004–0, Vienna, Austria July, 2004.

[IAEA, 2012] International Atomic Energy Agency, *The Safety Case and Safety Assessment for the Disposal of Radioactive Waste*, Specific Safety Guide No. SSG-23, STI/PUB/1553, Vienna, September 2012.

[Kearsley, 2002] Kearsleya, EP, PJ Wainwright, *The effect of porosity on the strength of foamed concrete*, Cement and Concrete Research, 32, p233–239.

[Kellett, 2009] Kellett MA, Bersillon O, Mills RW, *The JEFF-3.1/-3.1.1 radioactive decay data and fission yields sub-libraries*, JEFF Report 20, ISBN 978-92-64-99087-6, OECD/NEA No. 6287, Paris, 2009, 1-147.

[Kursten, 2015] Kursten B, F Druyts, *Assessment of the uniform corrosion behaviour of carbon steel radioactive waste packages with respect to the disposal concept in the geological Dutch Boom Clay formation*, OPERA report OPERA-PU-SCK513, May 2015, 1-107.

[Marivoet; 2012] Marivoet J, *Treatment of actinide decay chains in safety assessment calculations*, DRAFT, SCK•CEN, 2012.

[Meeussen, 2003] Meeussen JCL, *ORCHESTRA: An Object-Oriented Framework for Implementing Chemical Equilibrium Models*, Environmental Science & Technology 37 (6), 1175-1182, 2003.

[Meeussen, 2014] Meeussen JCL, Rosca-Bocancea E, *Determination of the inventory: part B matrix composition*, OPERA report OPERA-PU-NRG1112B, December 2014.

[Meeussen, 2017a] Meeussen JCL, Rosca-Bocancea E, Schröder TJ, Koenen M, Valega Mackenzie F, Maes N, C. Bruggeman C, *Model representation of radionuclide migration in Boom Clay*, OPERA report OPERA-PU-NRG6131, February 2017.

[Meeussen, 2017b] Meeussen JCL, Rosca-Bocancea E, Schröder TJ, Koenen M, Valega Mackenzie F, Maes N, Bruggeman C, *Reference database with diffusion properties*, OPERA report OPERA-PU-NRG6132, February 2017.

[Meeussen, 2017c] Meeussen, JCL, JB Grupa, *Migration of radionuclides in Boom Clay, PA model 'Clay'- Annex 2D effects*, OPERA report OPERA-PU-NRG7214, submitted.

[Nagra, 2002] National Cooperative for the Disposal of Radioactive Waste (Nagra), *Project Opalinus Clay. Safety Report. Demonstration of disposal feasibility for spent fuel, vitrified high-level wasteand long-lived intermediate-level waste (Entsorgungs-nachweis)*, Nagra technical report 02-05, 2002, 1-471.

[NEA, 2004] Nuclear Energy Agency, *Post-closure Safety Case for Geological Repositories: Nature and Purpose*, NEA Report No. 3679, OECD/NEA, Paris, France, 2004.

[NEA, 2012] Nuclear Energy Agency, *Indicators in the Safety Case – A report of the Integrated Group on the Safety Case (IGSC)*, NEA/RWM/R(2012)7, 2012.

[Neeft, 2017] Neeft, E, e-mail communication 24-1-2017.

[ONDRAF/NIRAS, 2009] ONDRAF/NIRAS, The Long-term Safety strategy for the geological disposal of radioactive waste, NIROND-TR-2009-12E, 2009.

[Rosca-Bocancea, 2016] Rosca-Bocancea E, Schröder TJ, *Development of Safety and Performance Indicators*, OPERA-PU-NRG7311, January 2016.

[Rosca-Bocancea, 2017] Rosca-Bocancea A, J.C.L. Meeussen JCL, *Modelling of radionuclide migration in the rock formations surrounding the host rock*, OPERA report OPERA-PU-NRG7223, submitted.

[Rijkswaterstaat, 2016] Rijkswaterstaat, *Waternormalen*, *https://staticresources.rijkswaterstaat.nl/binaries/Referentiewaarden%20afvoeren_tcm174-326694_tcm21-24221.pdf*, last accessed 26 July 2016.

[Salah, 2014] Salah, S, L Wang, *Speciation and solubility calculations for waste relevant radionuclides in Boom Clay*, SCK·CEN report ER-198, 2014, 1-153.

[Schelland, 2014] Schelland M, Hart J, Wildenborg AFB, Grupa JB, *OPERA FEP-database*, OPERA report OPERA-PU-TNO2123A, June 2014.

[Schröder, 2016] Schröder T J, Rosca-Bocancea E, *Safety and performance indicator calculation methodology*, OPERA-PU-NRG7312, January 2016.

[Schröder, 2017a] Schröder TJ, Meeussen JCL, Dijkstra JJ, Bruggeman C, Maes N, *Report on model representation of radionuclide sorption in Boom Clay*, OPERA report OPERA-PU-NRG6121, January 2017.

[Schröder, 2017b] Schröder TJ, Meeussen JCL, Dijkstra JJ, *Final report on radionuclide sorption in Boom Clay*, OPERA report OPERA-PU-NRG6123, February 2017.

[Schröder, 2017c] Schröder TJ, Meeussen JCL, Rosca-Bocancea, E, *Solubility limits in the Waste-EBS and Host Rock*, OPERA report OPERA-PU-NRG742, to be submitted.

[Valstar, 2017] Valstar JR, Goorden N, *Hydrological transport in the rock formations surrounding the host rock*, OPERA report OPERA-PU-DLT621, 2017.

[Ten Veen, 2015] Ten Veen J, Govaerts J, Beerten K, Ventra D, Vis G, *Future evolution of the geological and geohydrological properties of the geosphere*, OPERA report OPERA-PU-TNO412, 2015, 1-121.

[Verhoef, 2011] Verhoef E, Schröder TJ, *Research Plan*, OPERA report OPERA-PG-COV004, COVRA N.V., 2011.

[Verhoef, 2014a] Verhoef E, Neeft E, Grupa, J, Poley A, *Outline of a disposal concept in clay, First update*, OPERA report OPERA-PG-COV008, 13 november 2014, 1-20.

[Verhoef, 2014b] Verhoef E, AMG de Bruin, RB Wiegers, EAC Neeft, G Deissmann, *Cementitious materials in OPERA disposal concept in Boom Clay*, OPERA report OPERA-PG-COV020, 30 April 2014, 1-20.

[Verhoef, 2015] Verhoef EV, Neeft EAC, Deissmann G, Filby A, Wiegers RB, Kers DA, *Waste families in OPERA*, OPERA report OPERA-PG-COV023, September 2015.

[Verhoef, 2016] Verhoef, E, e-mail communication, 20 December 2016.

[Vis, 2014] Vis G-J, Verweij JM, *Geological and geohydrological characterization of the Boom Clay and its overburden*, OPERA report OPERA-PU-TNO411, March 2014.

[Wang, 2013] Wang, L, *Solubility of radionuclides in Supercontainer concrete. Transferability document: Use of solubility determined within the category A (cAt) project in the B&C waste disposal assessment*, SCK·CEN report ER-239, 2013, 1-43.

Appendix 1 Overview of Disposal Galleries

Table A-1 contains an overview of the geometric dimensions and numbers of disposal galleries of the OPERA disposal concept, based on a critical evaluation of the number of containers that may be stacked inside a gallery and the gallery length that are necessary to do so. The geometry is based on [Verhoef, 2014a] and the number of waste containers is reported in [Verhoef, 2015]. The estimated porosities are summarized in Table 3-2, and the resulting pore volumes and footprint areas are reported in Table 3-3.

Table A-1: Evaluation of required disposal galleries

Disposal Section	Waste Canister [-]	Excavated diameter of gallery [m]	Dimension of waste package (*d* x *l* or *l* x *h* x *w*) [m]	Number of waste packages [-]	Number of galleries [-]	Effective gallery length* [m]
Vitrified HLW	CSD-V	3.2	1.9 x 2.5	487	32	40
Spent Fuel	ECN	3.2	1.9 x 3.0	75	6	40
Non-heat-generating HLW	CSD-C	3.2	1.9 x 2.5	600	38	40
	ECN		1.9 x 3.0	100	8	
DepU	Konrad	4.8	1.7 x 1.6 x 1.7	9060	38	190
LILW	200 l	4.8	0.59 x 0.88	140’000	25	190
	1000 l		1.0 x 1.25	12’000	10	

* exclusive disposal gallery seal

Appendix 2 Radionuclide sorption parameter for Boom Clay

Table A-2: Ranges of calculated K_d- and R-values in Boom Clay of the Netherlands for the *base case* (CV, 100 mg/l DOC). Lower, central, and upper values correspond to 5-, 50- and 95-percentiles of the calculated values, respectively.

Element	$K_{d\text{-}diss}$			$K_{d\text{-}DOC}$			R_{dis}			R_{DOC}		
	lower	central	upper	lower	central	upper	lower	central	upper	lower	central	upper
Se	0	0	0	51	129	247	1	1	1	236	621	1263
U	7	>10’000	>10’000	16	46	95	33	>50’000	>50’000	77	221	489
Tc	>10’000	>10’000	>10’000	16	46	95	>50’000	>50’000	>50’000	77	221	489
Th	>10’000	>10’000	>10’000	16	46	95	>50’000	>50’000	>50’000	77	221	489
Np	>10’000	>10’000	>10’000	16	46	95	>50’000	>50’000	>50’000	77	221	489
K	0	7	387	113	485	1068	3	34	1997	525	2300	5694
Cd	>10'000	>10'000	>10'000	16	46	95	>50'000	>50'000	>50'000	78	222	490
Ca	9	1114	>10’000	133	603	1831	46	5409	>50’000	611	2881	9584
Pu	>10’000	>10’000	>10’000	16	46	95	>50’000	>50’000	>50’000	77	221	489
Am	>10’000	>10’000	>10’000	24	71	366	>50’000	>50’000	>50’000	116	349	1676
Sn	>10’000	>10’000	>10’000	16	46	95	>50’000	>50’000	>50’000	77	221	489
Eu	>10’000	>10’000	>10’000	20	56	146	>50’000	>50’000	>50’000	95	267	706
Ni	>10’000	>10’000	>10’000	17	47	96	>50’000	>50’000	>50’000	81	227	494
Cs	103	1329	7596	3413	>10’000	>10’000	476	6454	38’699	16611	>50’000	>50’000
Cm	>10’000	>10’000	>10’000	16	46	95	>50’000	>50’000	>50’000	78	222	489
Sr	33	2762	>10’000	35	95	273	160	13’329	>50’000	161	461	1375
Ra	18	1554	>10’000	34	95	275	87	7320	>50’000	161	458	1364
Pb	>10’000	>10’000	>10’000	25	69	237	>50’000	>50’000	>50’000	120	338	1145

Table A-3: Ranges of calculated K_d- and R-values in Boom Clay of the Netherlands for the *low DOC case* (LD, 20 mg/l DOC). Lower, central, and upper values correspond to 5-, 50- and 95-percentiles of the calculated values, respectively.

Element	$K_{d\text{-}diss}$			$K_{d\text{-}DOC}$			R_{dis}			R_{DOC}		
	lower	central	upper	lower	central	upper	lower	central	upper	lower	central	upper
Se	0	0	0	257	646	1235	1	1	1	1178	3100	6311
U	7	>10’000	>10’000	81	231	473	33	>50’000	>50’000	382	1103	2442
Tc	>10’000	>10’000	>10’000	81	231	473	>50’000	>50’000	>50’000	382	1103	2442
Th	>10’000	>10’000	>10’000	81	231	473	>50’000	>50’000	>50’000	382	1103	2442
Np	>10’000	>10’000	>10’000	81	231	473	>50’000	>50’000	>50’000	382	1103	2442
K	0	7	387	567	2423	5339	3	34	1996	2619	11496	28464
Cd	>10'000	>10'000	>10'000	82	232	474	>50'000	>50'000	>50'000	386	1106	2445
Ca	9	1114	>10’000	663	3016	9153	46	5400	>50’000	3051	14’398	47’917
Pu	>10’000	>10’000	>10’000	81	231	473	>50’000	>50’000	>50’000	382	1103	2442
Am	>10’000	>10’000	>10’000	119	357	1829	>50’000	>50’000	>50’000	578	1741	8379
Sn	>10’000	>10’000	>10’000	81	231	473	>50’000	>50’000	>50’000	382	1103	2442
Eu	>10’000	>10’000	>10’000	100	278	732	>50’000	>50’000	>50’000	473	1332	3527
Ni	>10’000	>10’000	>10’000	86	236	481	>50’000	>50’000	>50’000	402	1130	2468
Cs	103	1328	7594	>10’000	>10’000	>10’000	476	6453	38’699	>50’000	>50’000	>50’000
Cm	>10’000	>10’000	>10’000	82	231	473	>50’000	>50’000	>50’000	384	1105	2442
Sr	33	2761	>10’000	173	474	1365	160	13’289	>50’000	802	2303	6873
Ra	18	1550	>10’000	173	475	1373	87	7315	>50’000	799	2287	6816
Pb	>10’000	>10’000	>10’000	125	347	1184	>50’000	>50’000	>50’000	595	1685	5722

Table A-4: Ranges of calculated K_d- and R-values in Boom Clay of the Netherlands for the *high DOC case* (HD, 200 mg/l DOC). Lower, central, and upper values correspond to 5-, 50- and 95-percentiles of the calculated values, respectively.

Element	$K_{d\text{-}diss}$			$K_{d\text{-}DOC}$			R_{dis}			R_{DOC}		
	lower	central	upper	lower	central	upper	lower	central	upper	lower	central	upper
Se	0	0	0	26	65	123	1	1	1	119	311	632
U	7	27000	1.41E+08	8	23	47	33	>50’000	>50’000	39	111	245
Tc	>10’000	>10’000	>10’000	8	23	47	>50’000	>50’000	>50’000	39	111	245
Th	>10’000	>10’000	>10’000	8	23	47	>50’000	>50’000	>50’000	39	111	245
Np	>10’000	>10’000	>10’000	8	23	47	>50’000	>50’000	>50’000	39	111	245
K	0	7	387	57	242	534	3	34	1999	263	1151	2847
Cd	>10'000	>10'000	>10'000	8	23	47	>50'000	>50'000	>50'000	39	111	245
Ca	9	1114	>10’000	66	302	915	46	5427	>50’000	306	1441	4793
Pu	>10’000	>10’000	>10’000	8	23	47	>50’000	>50’000	>50’000	39	111	245
Am	>10’000	>10’000	>10’000	12	36	183	>50’000	>50’000	>50’000	58	175	838
Sn	>10’000	>10’000	>10’000	8	23	47	>50’000	>50’000	>50’000	39	111	245
Eu	>10’000	>10’000	>10’000	10	28	73	>50’000	>50’000	>50’000	48	134	353
Ni	>10’000	>10’000	>10’000	9	24	48	>50’000	>50’000	>50’000	41	114	248
Cs	103	1329	7597	1706	>10’000	>10’000	476	6457	38’699	8302	>50’000	>50’000
Cm	>10’000	>10’000	>10’000	8	23	47	>50’000	>50’000	>50’000	39	111	245
Sr	34	2764	>10’000	17	47	136	160	13’382	>50’000	81	231	688
Ra	18	1557	>10’000	17	47	137	87	7330	>50’000	81	230	682
Pb	>10’000	>10’000	>10’000	12	35	118	>50’000	>50’000	>50’000	60	169	573

Disclaimer

OPERA

Meer informatie:

Postadres
Postbus 202
4380 AE Vlissingen

T 0113-616 666
F 0113-616 650
E info@covra.nl

www.covra.nl